Biochemical Pharmacology 199 (2022) 115007

Contents lists available at ScienceDirect

Biochemical Pharmacology

journal homepage: www.elsevier.com/locate/biochempharm

Pretreatment of umbilical cord derived MSCs with IFN-γ and TNF-α enhances the tumor-suppressive effect on acute myeloid leukemia

Luchen Sun [a], Jingyue Wang [a], Qiuping Wang [a], Zhonglei He [c], Tingzhe Sun [d], Yongfang Yao [a], Wenxin Wang [c], Pingping Shen [a,b,*]

[a] State Key Laboratory of Pharmaceutical Biotechnology, School of Life Sciences, Nanjing University, Nanjing 210023, China
[b] Shenzhen Research Institute of NanJing University, Shenzhen 518000, China
[c] Charles Institute of Dermatology, School of Medicine, University College Dublin, Dublin, Ireland
[d] School of Life Sciences, Anqing Normal University, Anqing 246133, China

ARTICLE INFO

Keywords:
AML
UC-MSCs
TRAIL
IDO
Pretreatment

ABSTRACT

Currently, the standard therapeutic approach of AML consists of chemotherapy and allogeneic hematopoietic stem cell transplantation (HSCT). However, these strategies are usually associated with adverse side effects and high risk of relapse following HSCT. Thus, it is imperative to find an alternative way against AML progression. Here, we showed that treatment with umbilical cord-derived mesenchymal stem cells (UC-MSCs) could efficiently induce apoptosis in both primary AML patient-derived leukemic cells and AML cell lines. Mechanistically, tumor necrosis factor-α-related apoptosis-inducing ligand (TRAIL) in UC-MSCs mediated the proapoptotic effect in AML cells. Besides, indoleamine 2,3-dioxygenase (IDO) secreted by UC-MSCs blocked the cell cycle progression and inhibited the proliferation of AML cells. Importantly, we found that incubation of UC-MSCs with IFN-γ and TNF-α could upregulate the expression of TRAIL and IDO, resulting in an intensive pro-apoptotic efficacy. UC-MSCs pre-treatment could not only relieve the AML burden but also eliminate AML cells in a xenograft AML model. Our findings have shed light on an effective pre-activated approach to aggravating the anti-leukemia effect of MSC. Furthermore, a novel and safe stem cell-based therapy approach for AML treatment.

1. Introduction

Acute myeloid leukemia (AML) is a blood malignancy characterized by the accumulation of a large number of uncontrolled myeloid immature cells in peripheral blood and bone marrow [1,2]. The accumulation of these immature hematopoietic precursor cells can impair the normal hematopoietic function and lead to bone marrow hyperplasia, hepatosplenomegaly, fever, anemia, liver and kidney failure [3-5]. The only curative therapeutic approach for AML is allogeneic stem cell transplantation (HSCT) combined with high-dosage chemotherapy [6,7], whereas the intensive chemotherapy often produces adverse effects and HSCT is not suitable for specific patients [8,9]. Relapse following the conventional treatment is the major challenge and is correlated with poor prognosis [10-12]. Currently, although CD19-targeted chimeric antigen receptor (CAR)-T cell therapies have achieved remarkable clinical success in B-lymphoid malignancies, CAR-T therapies for AML have failed in clinical trials due to tedious manufacturing strategies and the absence of a dispensable antigen, resulting in intolerable myeloablation [13-15]. Therefore, there is an urgent need to develop novel therapeutic approaches for AML treatment.

Mesenchymal stem cells (MSCs) are a kind of multipotent cells, which are widely distributed in the umbilical cord, fat, bone marrow and other tissues. Studies have demonstrated a tumoricidal effect of MSCs on tumor growth by secreting cytokines, exosomes or miRNAs [16,17]. In addition, MSCs can also migrate to tumor areas and subsequently induce cell cycle arrest or apoptosis in tumor cells. For instance, Qiao et al. reported that human MSCs inhibited breast cancer cell proliferation through the Wnt pathway [18]. Lee et al. reported that human bone marrow MSCs incubated with TNF-α upregulated the expression of tumor necrosis factor-α-related apoptosis-inducing ligand (TRAIL) and induced apoptosis of breast cancer cells in an MDA-MB-231 xenograft mice model [19]. Till now, MSC-based cell therapy has been widely used

Abbreviations: MSC, mesenchymal stem cell; AML, acute myeloid leukemia; TRAIL, tumor necrosis factor-a-related apoptosis-inducing ligand; IDO, indoleamine 2,3-dioxygenase; TNF-α, tumor necrosis factor-α; IFN-γ, Interferon-gamma.

* Corresponding author at: State Key Laboratory of Pharmaceutical Biotechnology, School of Life Sciences, Nanjing University, Nanjing 210023, China.
E-mail address: ppshen@nju.edu.cn (P. Shen).

https://doi.org/10.1016/j.bcp.2022.115007
Received 15 January 2022; Received in revised form 9 March 2022; Accepted 13 March 2022
Available online 17 March 2022
0006-2952/© 2022 Elsevier Inc. All rights reserved.

to treat various malignant diseases. Many clinical trials for treatment of hematologic malignancies using MSCs are registered at https://www.clinicaltrials.gov, including AML (NCT02181478, NCT03096782). MSCs have been shown to suppress lymphoma and leukemia cell proliferation *in vitro* [20]. Zhu and colleagues reported that MSCs inhibited growth of chronic myeloid leukemia by secreting Dickkopf related protein 1 (DKK-1) [21]. Only a few reports have indicated that MSCs can promote apoptosis of hematologic malignant cells [22]. However, the underlying anti-cancer mechanisms of MSCs in hematologic malignancies remain unclear.

In current study, we demonstrated that umbilical cord derived MSCs (UC-MSCs) have tumor suppressive effects on AML cells. Mechanistically, we found that UC-MSCs could upregulate TRAIL and promote AML apoptosis. Moreover, UC-MSCs restrained the cell cycle of AML cells at G0/G1 phase by secreting indoleamine 2,3-dioxygenase (IDO). Interestingly, our data showed that IFN-γ and TNF-α secreted by AML cells could activate UC-MSCs, leading to increased expression of TRAIL and IDO. Thus, pretreatment of UC-MSCs with IFN-γ and TNF-α inhibited cell cycle progression and promoted apoptosis in AML cells. In an AML xenograft model, primed UC-MSCs reduced the tumor burden *in vivo* and prolonged the survival of AML mice. Collectively, we have provided a novel MSC-based approach for the anti-AML treatment.

2. Materials and methods

2.1. Reagents and antibodies

2.2. Cell culture

Primary leukemia cells and umbilical cord mesenchymal stem cells (UC-MSCs) from healthy donors were obtained from Nanjing Drum Tower Hospital (Nanjing, China) after informed consent was obtained. U937 and THP-1 cells were obtained from China Center for Type Culture Collection (CCTCC, Wuhan, China) and were cultured in the RPMI 1640 medium. All media were supplemented with 1% penicillin-streptomycin and 10% fetal bovine serum. The cells were kept in a humidified atmosphere of 5% CO_2 at 37 °C.

2.3. Differentiation of UC-MSCs

Adipogenic and osteogenic differentiation were induced *in vitro*, and UC-MSCs identification was carried out. To achieve adipogenic differentiation, we used two kinds of media. Firstly, UC-MSCs were cultured with 5 μM dexamethasone, 0.5 mM Isobutylmethylxanthine (IBMX), 850 nM insulin, 1 nM Triiodothyronine (T3), 1 μM rosiglitazone and 125 nM indomethacin in DMEM plus 10% FBS. The induction differentiation medium was replaced with the maintenance medium at 48 h, which included 850 nM insulin, 1 nM T3, 1 μM rosiglitazone. The culture medium was changed alternately until lipid droplets formed. After 8 days, adipocytic differentiation was examined through oil red O staining. Osteogenic MSC differentiation was performed with conditional medium containing 0.1 μM dexamethasone, 10 mM β-glycerophosphate disodium, and 10 μg/ml vitamin C. The medium was changed every other day. Two weeks later, UC-MSCs were stained with alizarin red to examine calcium deposition.

2.4. Quantitative real-time PCR (RT-qPCR)

Total RNA was extracted using TRIzol (Invitrogen). Reverse transcription was performed with a 5 × All-In-One RT Master Mix (Abcam) kit, and quantitative PCR reactions were performed using SYBR Green Master Mix (Vazyme biotech) kit. PCRs were performed in a total volume of 20 μl. Data were collected and analyzed by CFX96 Real-Time System (Bio-Rad C1000 Touch Thermal Cycler Real-Time PCR System). The details of primers are listed as follows.

2.5. Cell cycle, apoptosis and flow cytometry analysis

To evaluate cell cycling, co-cultured U937 or THP-1 cells were fixed with 70% ethanol in PBS at −20 °C overnight. Propidium iodide (Sigma) was used as a nucleic acid dye. The apoptotic cells were measured by Annexin V/PI according to manufacturer's protocol (BD Biosciences). The cells were analyzed on BD FACSCalibur cytometer using CellQuest software (BD Biosciences). The data were analyzed using FlowJo software. The statistics presented are derived from at least 10,000 events from the gated population of interest.

2.6. CRISPR-Cas9 knockout

Cas9/TRAIL MSC were constructed with lentiCRISPR v2 (Addgene #52961) lentivirus containing Cas9, a puromycin resistance gene, and the following CRISPR sgRNA guide sequences: TRAIL (GCCACUUGACUUGCCAGCAG); HEK293T cells were seeded in cell culture dish and transfected with the plasmid mixture of the lentivirus vector, using Lipofectamine 2000 (Thermo Fisher Scientific), according to the manufacturer's instruction. Supernatant containing the lentivirus was collected 48 and 72 h after transfection and filtered with 0.45 mm filters. Following the collection of the virus, DNA plasmids were transfected into UC-MSCs. After 48 h, infected cells were selected Blasticidin (10 mg/ml). Single clonal cells were obtained by limiting dilution method.

2.7. Western blotting

The cells were extracted by cell lysis buffer purchased from Beyotime, which contained 1 × protease inhibitors (MCE). The cell debris were removed by centrifugation at 4 °C, and the supernatants were collected and stored at −80 °C until use. The total protein concentration of serum was determined by the Pierce BCA assay. The protein was electrophoresed on SDS-polyacrylamide gels and then electrotransferred onto a polyvinylidene fluoride membrane (Sigma). A quantity of 5% non-fat milk in TBST was used to block the membranes and then incubated with primary antibodies as indicated. HRP-conjugated anti-rabbit/mouse IgG was used as secondary antibody. Chemiluminescence signal was developed with Thermo Scienfitic Super Signal West Femto Maximum Sensitivity Substrate and detected by Fluorescence & Chemiluminescence Imaging System (Tanon). Densitometry with Image-pro plus software was used for quantifying the intensities of stained bands.

2.8. Enzyme linked immunosorbent assay (ELISA)

UC-MSCs were seeded at a density of 1×10^5 cells/mL in a 12-well plate cultured for 24 h before use. U937 and THP-1 cells were added to UC-MSCs for 1 or 2 days then the supernatants were collected. The levels of IFN-γ and TNF-α in the supernatants were detected by ELISA (PeproTech) following protocols suggested by the manufacturer.

2.9. Cell counting kit 8 (CCK8) assay

U937 and THP-1 cell suspensions of 100 μl at the concentration of 1×10^5 cells/ml were inoculated in a 96-well plate and cocultured with UC-MSCs culture supernatant (control without UC-MSCs culture supernatant) for 24 or 48 h. Then, 10 μl of CCK8 solution was added to each well, followed by 2 h of incubation at 37 °C. The absorbance was measured at 450 nm, each group had three repeats, and the experiment was repeated three times.

2.10. Determination of IDO enzyme activity

Kynurenine levels were measured to determine IDO enzyme activity as previously described [23]. In brief, 100 μl of MSC supernatant was

Reagent or Resource	Source	Identifier
Antibodies		
CD73-FITC	eBioscience, USA	11-0739-41
CD90-FITC	eBioscience, USA	11-0909-41
CD105-PE	eBioscience, USA	12-1057-41
CD14-PerCP-Cy5.5	BD Biosciences, USA	7187547
CD34-FITC	BD Biosciences, USA	4364560
CD45-FITC	eBioscience, USA	11-9459-41
Bax	Beyotine, China	AB026-1
Bcl-2	Bioworld, USA	BS1511
PARP	Cell Signaling Technology, USA	9532S
TRAIL	Cell Signaling Technology, USA	3219S
cyclin D1	Bioss, China	bs-0572R
p21	Santa Cruz Biotechnology, USA	sc-6246
Caspase-3	Proteintech Group, USA	19677-1-AP
Caspase-8	Proteintech Group, USA	13423-1-AP
Caspase-9	Cell Signaling Technology, USA	9508S
Actin-HRP conjugated	Zen Bioscience, China	700068
GAPDH-HRP conjugated	Bioworld, USA	MB001H
Reagents		
Penicillin and streptomycin	Beyotime, China	C0222
TRIzol	Invitrogen, USA	15596-018
5× All-In-One RT Master Mix	Abcam, USA	AAS946
SYBR Green Master Mix	Vazyme biotech, China	Q111-03
protease inhibitors	MedChemExpress, USA	HY-K0010
DAPI	Beyotime, China	C1002
CFDA SE	Beyotime, China	C1031
Earlich's reagent	Sigma, USA	156477
Propidium iodide	Sigma, USA	P4170
Blasticidin	MedChemExpress, USA	HY-103401
Alizarin Red	Sigma, USA	A5533
oil red O	Sigma, USA	O0625
NLG919	MedChemExpress, USA	HY-18770B
Cytarabine	MedChemExpress, USA	HY-13605
vitamin C	MedChemExpress, USA	HY-B0166
β-glycerophosphate disodium	MedChemExpress, USA	HY-D0886
Dexamethasone	MedChemExpress, USA	HY-14648
Isobutylmethylxanthine	MedChemExpress, USA	HY-12318
Indomethacin	MedChemExpress, USA	HY-14397
Insulin	MedChemExpress, USA	HY-P73243
Triiodothyronine	MedChemExpress, USA	HY-A0070A
Rosiglitazone	MedChemExpress, USA	HY-17386
Lipofectamine 2000	Thermo Fisher Scientific, USA	11668019
Annexin V-FITC/PI Apoptosis Detection Kit	Vazyme biotech, China	A211-01
Human IFN-γ ELISA Development Kit	PeproTech	900-TM27
Human TNF-α ELISA Development Kit	PeproTech	900-TM25
CCK-8 Cell Counting Kit	Vazyme biotech, China	A311-01
RPMI 1640	BasalMedia, China	L210KJ
α-MEM	BasalMedia, China	L560KJ
DMEM	BasalMedia, China	L110KJ
DMEM/F12	BasalMedia, China	L320KJ
Fetal bovine serum (FBS)	Gibco, USA	16140071

Gene	Sequences	
Fas-L	Forward Primer	TGCCTTGGTAGGATTGGGC
	Reverse Primer	GCTGGTAGACTCTCGGAGTTC
TRAIL	Forward Primer	TGCGTGCTGATCGTGATCTTC
	Reverse Primer	GCTCGTTGGTAAAGTACACGTA
APO3-L	Forward Primer	CCGTCCAGTTGGTGGGTAAC
	Reverse Primer	CCATCACGTCGTAGAGCTGC
Fas	Forward Primer	TCTGGTTCTTACGTCTGTTGC
	Reverse Primer	CTGTGCAGTCCCTAGCTTTCC
APO2	Forward Primer	GCGGGGAGGATTGAACCAC
	Reverse Primer	CGACGACAAACTTGAAGGTCTT
APO3	Forward Primer	CCGTCCAGTTGGTGGGTAAC
	Reverse Primer	CCATCACGTCGTAGAGCTGC
cyclin D1	Forward Primer	GCTGCGAAGTGGAAACCATC
	Reverse Primer	CCTCCTTCTGCACACATTTGAA
p21	Forward Primer	TGTCCGTCAGAACCCATGC
	Reverse Primer	AAAGTCGAAGTTCCATCGCTC
TGF-β	Forward Primer	GGCCAGATCCTGTCCAAGC
	Reverse Primer	GTGGGTTTCCACCATTAGCAC
HGF	Forward Primer	GCTATCGGGGTAAAGACCTACA
	Reverse Primer	CGTAGCGTACCTCTGGATTGC
IL-10	Forward Primer	GACTTTAAGGGTTACCTGGGTTG
	Reverse Primer	TCACATGCGCCTTGATGTCTG
IDO	Forward Primer	GCCAGCTTCGAGAAAGAGTTG
	Reverse Primer	ATCCCAGAACTAGACGTGCAA
MCP-1	Forward Primer	CAGCCAGATGCAATCAATGCC
	Reverse Primer	TGGAATCCTGAACCCACTTCT
CCL5	Forward Primer	CCAGCAGTCGTCTTTGTCAC
	Reverse Primer	CTCTGGGTTGGCACACACTT
CCR2	Forward Primer	CCACATCTCGTTCTCGGTTTATC
	Reverse Primer	CAGGGAGCACCGTAATCATAATC
CCR3	Forward Primer	TGGCATGTGTAAGCTCCTCTC
	Reverse Primer	CCTGTCGATTGTCAGCAGGATTA
CCR5	Forward Primer	TTCTGGGCTCCCTACAACATT
	Reverse Primer	TTGGTCCAACCTGTTAGAGCTA
CXCR4	Forward Primer	ACTACACCGAGGAAATGGGCT
	Reverse Primer	CCCACAATGCCAGTTAAGAAGA
CXCL12	Forward Primer	ATTCTCAACACTCCAAACTGTGC
	Reverse Primer	ACTTTAGCTTCGGGTCAATGC
CCL18	Forward Primer	TGCCCTCCTTGTCCTCGTCTG
	Reverse Primer	GTATAGACGAGGCAGCAGA
ANG	Forward Primer	CTGGGCGTTTTGTTGTTGGTC

(*continued on next page*)

supplemented with 25 μl of trichloroacetic acid 30% (vol/vol), vortexed, and incubated for 30 min at 50 °C to hydrolyze N-*formylkynurenine* to kynurenine. Then, after centrifugation for 10 min at 10,000*g*, 100 μl of supernatant was transferred into a 96-well flat-bottomed plate and mixed with an equal volume of 2% Ehrlich's reagent (Sigma). Following 10 min of incubation, absorbance was read at a 492 nm wavelength with a microplate reader.

2.11. Immunofluorescence

Immunofluorescence was performed as previously described [24]. The sections were blocked in phosphate-buffered saline (PBS) with 10% goat serum at room temperature for 1 h. After blocking, the sections were incubated with a primary antibody overnight at 4 °C. The sections were then briefly rinsed with PBS, washed 3 times for 5 min each time, and incubated with fluorescence-coupled secondary antibody for 4 h at room temperature. Nuclei staining was performed by incubating the cells with DAPI. The specimens were then observed at the appropriate fluorescence wavelength using a confocal microscope. Image analysis was done with Image-pro plus software.

2.12. Mice

Eight-week-old NOD-SCID mice were purchased from the Model Animal Research Center of the Nanjing University, Nanjing, China, and housed in our animal facilities under specific pathogen-free conditions. All mouse procedures and experiments for this study were approved by the Institutional Animal Care and Use Committee at Nanjing University (ICAUC-2007021). The average weight of the mice at the start of the experiment was 25 g. Vendor health reports indicated that the mice were free of known viral, bacterial, and parasitic pathogens. All animals were either treated (where possible) or humanely euthanized at any sign of

(*continued*)

	Reverse Primer	GGTTTGGCATCATAGTGCTGG
IGFBP4	Forward Primer	GGTGACCACCCCAACAACAG
	Reverse Primer	GGTGACCACCCCAACAACAG
NTF3	Forward Primer	CCGTGGCATCCAAGGTAACAA
	Reverse Primer	GCAGTTCGGTGTCCATTGC
galectin	Forward Primer	TCGCCAGCAACCTGAATCTC
	Reverse Primer	GCACGAAGCTCTTAGCGTCA
IL-17a	Forward Primer	TCCCACGAAATCCAGGATGC
	Reverse Primer	GGATGTTCAGGTTGACCATCAC
CHI3L1	Forward Primer	GTGAAGGCGTCTCAAACAGG
	Reverse Primer	GAAGCGGTCAAGGGCATCT
IL-6	Forward Primer	ACTCACCTCTTCAGAACGAATTG
	Reverse Primer	CCATCTTTGGAAGGTTCAGGTTG
DKK1	Forward Primer	CCTTGAACTCGGTTCTCAATTCC
	Reverse Primer	CAATGGTCTGGTACTTATTCCCG
PERP	Forward Primer	CTTCACCCTTCATGCCAACC
	Reverse Primer	GCCAATCAGGATAATCGTGGCT
PRNP	Forward Primer	AGTCAGTGGAACAAGCCGAG
	Reverse Primer	CTGCCGAAATGTATGATGGGC
PHLDA1	Forward Primer	GAAGATGGCCCATTCAAAAGCG
	Reverse Primer	GAGGAGGCTAACACGCAGG
XIAP	Forward Primer	ACCGTGCGGTGCTTTAGTT
	Reverse Primer	TGCGTGGCACTATTTTCAAGATA
NET1	Forward Primer	GAGCCAAGCAATAAAAGAGTTCG
	Reverse Primer	TGGGACTGTTGACCTGCTAGA
TNFRSF1A	Forward Primer	TCACCGCTTCAGAAAACCACC
	Reverse Primer	GGTCCACTGTGCAAGAAGAGA

illness or stress.

2.13. Animal study

All animals were assessed to be healthy and free of disease prior to U937 cells implantation. Mice were randomly divided into saline group, MSC group, Pre-act MSC group and cytarabine group (6 in each group). Each mouse was intravenously injected with U937 cells suspension in logarithmic growth phase by 1×10^7 cells/group. After 7 days, the mice accepted treatment with MSC, Pre-act MSC (1×10^6, 1 time/week), saline or cytarabine (10 mg/kg, 5 times/week) separately. At the days of 21, mice were euthanized, leukemia cells in the peripheral blood and bone marrow were tested by FACS. The tissues of mice were collected and histological examination was performed.

2.14. Hematoxylin and eosin (HE) staining

Fixed paraffin-imbedded tissue slices from kidney, liver, spleen and lung were subjected to H&E staining and pathologic examination. After deparaffinization and rehydration, tissue sections were stained with hematoxylin solution for 5 min followed by 5 dips in 1% acid ethanol (1% HCl in 75% ethanol) and then rinsed in distilled water. Then the sections were stained with eosin solution for 3 min and followed by dehydration with graded alcohol and clearing in xylene. The mounted slides were then examined and photographed using a LEICA DM3000 LED.

2.15. Statistical analysis

Data were expressed as mean ± standard error of mean (SEM). Statistical analysis was performed by Student's *t*-test when comparison was made between two independent groups. ANOVA followed by Tukey's multiple comparison was used when three or more groups were involved. $p < 0.05$, $p < 0.01$, $p < 0.001$, and $p < 0.0001$ were considered statistically significant and marked by *, **, ***, or ****, respectively.

3. Results

3.1. UC-MSCs promote the apoptosis of AML cell

Umbilical cord-derived MSCs (UC-MSCs, hereafter called MSC) were characterized by the attached well-spread fibroblastic morphology (Fig. 1A). Moreover, MSC were positive for CD73, CD90 and CD105 expression, and were negative for CD14, CD34, CD45, as confirmed by flow cytometry analysis (Fig. 1B). In osteogenic or adipogenic induction media, MSC were differentiated into adipocytes, osteocytes, measured by Alizarin Red (Fig. 1C) or oil red O staining (Fig. 1D).

To test the impact of MSC on prompting the apoptosis of leukemia cells, two AML cell lines (U937, THP-1 cells) were cultured in the presence or absence of MSC for 24 or 48 h, and apoptosis was evaluated by annexin V/PI double staining. Flow cytometry analysis showed that MSC induced a significant elevation in annexin V/PI dual positive fractions progressively, accompanied by increased early apoptotic cells (Fig. 2A-B), suggesting that MSC promoted apoptosis of AML cells.

One hallmark of apoptosis is the high Bax/Bcl-2 ratio, which acts as a rheostat to determine the apoptotic susceptibility [25,26]. To verify that the cell death induced by MSC was owing to apoptosis, THP-1 cells were treated with MSC for 1–3 days, and the expression of Bax, Bcl-2 and PARP were quantified by western blot. The results showed that Bax expression was significantly increased, whereas Bcl-2 levels were not changed, leading to a higher Bax/Bcl-2 ratio (Fig. 2C). Moreover, the cleaved PARPs were also observed in MSC-treated THP-1 cells. The pro-PARP protein was gradually reduced, and the cleaved PARP was significantly increased (Fig. 2D). Consistently, the expressions of

apoptosis-related proteins were also time-dependent. However, the pro-apoptotic effect of MSCs was not observed in indirect co-culture (Fig. 2E-F). Taken together, these results suggested that MSC advanced the apoptosis of AML cells and this effect was dependent on cell-to-cell contact.

3.2. TRAIL mediates MSC-induced apoptosis of AML cells

Next, we sought to investigate the mechanism involved in MSC-induced apoptosis. As shown in Fig. 3A, THP-1 cells aggregated around MSC in the coculture, indicating that MSC could recruit AML cells to its surroundings. Recent studies have shown that MSC secreted chemokines, such as MCP-1, CCR2 and CXCL14, to recruit lymphocytes and endothelial cells to repair injuries and support wound healing [27-29]. Thus, we speculated that these chemokines were involved in the interaction between MSC and AML cells, and then examined the expressions of these chemokines and their corresponding receptors in MSC and THP-1 cells. The results revealed that compared with untreated cells, the expressions of chemokine MCP-1, CCL5 and chemokine receptors CCR2, CCR3 and CXCR4 were significantly increased in MSC (Fig. 3C). Meanwhile, the expressions of MCP-1, CCL5 and CCR3 were significantly increased in THP-1 cells (Fig. 3B). These data suggested that the interactions between MCP-1/CCR2 and CCL5/CCR3 might contribute to the *in vivo* mechanism of MSC action. Since physical contact was required for the pro-apoptotic effect of MSC, it is possible that the apoptosis-inducing ligands and their corresponding receptors expressed on the cell surface might participate in MSC-induced cell apoptosis. To verify this hypothesis, we employed RT-qPCR to determine the expressions of apoptosis-inducing ligands in tumor necrosis factor family and their receptors in MSC and THP-1 cells. As illustrated in Fig. 3D-E, the expression of tumor necrosis factor related apoptosis-inducing ligand (TRAIL) mRNA was dramatically elevated in MSC, accompanied by increased production of TRAIL receptor (APO2) in THP-1 cells. Consistently, western blotting showed increased TRAIL expression in MSC when incubated with U937 cells (Fig. 3F) and THP-1 cells (Fig. 3G).

To evaluate the role of TRAIL in controlling the viability of AML cells, antibody neutralization experiment was performed. We found that treatment with TRAIL neutralizing antibodies substantially diminished the apoptosis in U937 and THP-1 cells (Fig. 3H), implying that MSC promoted AML cell apoptosis via TRAIL. To further confirm the involvement of TRAIL in MSC-induced apoptosis in AML cells, CRISPR/

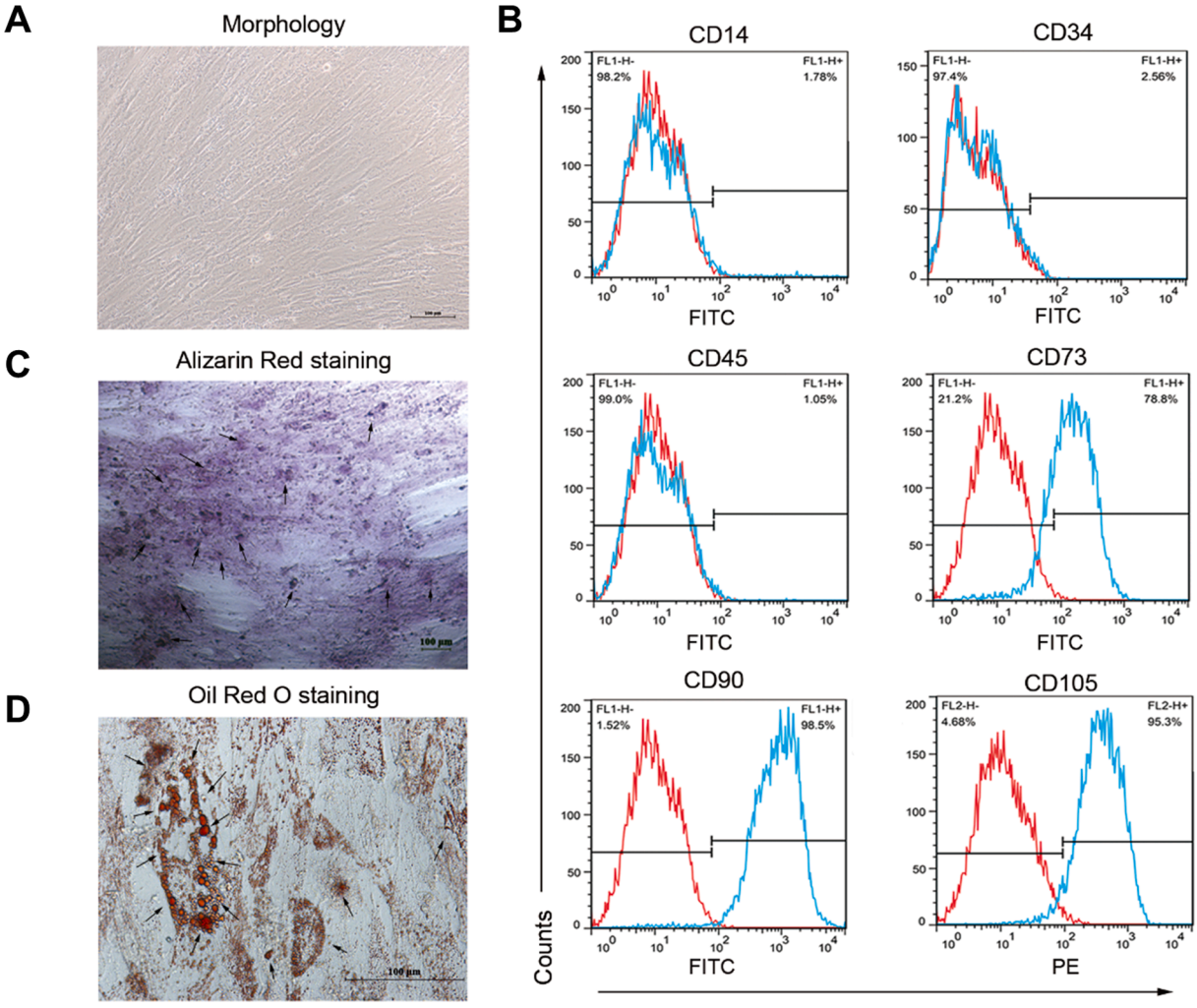

Fig. 1. The characteristics of umbilical cord derived from mesenchymal stem cell. (A) The morphology of UC-MSCs was observed by inverted microscopy. UC-MSCs with a fibroblast-like appearance with extensions in opposite directions from a small cell body (20×). (B) Flow cytometry analysis of cell surface markers on UC-MSCs. Positive markers were CD73, CD90, and CD105; cells were negative for CD14, CD34 and CD45. The red curves indicate the corresponding negative IgG isotype control antibodies. (C) Representative alizarine red S staining photomicrographs of UC-MSCs treated by the osteogenic differentiation medium. (D) Representative Oil Red staining photomicrographs of MSC treated by the adipogenic differentiation medium. (For interpretation of the references to colour in this figure legend, the reader is referred to the web version of this article.)

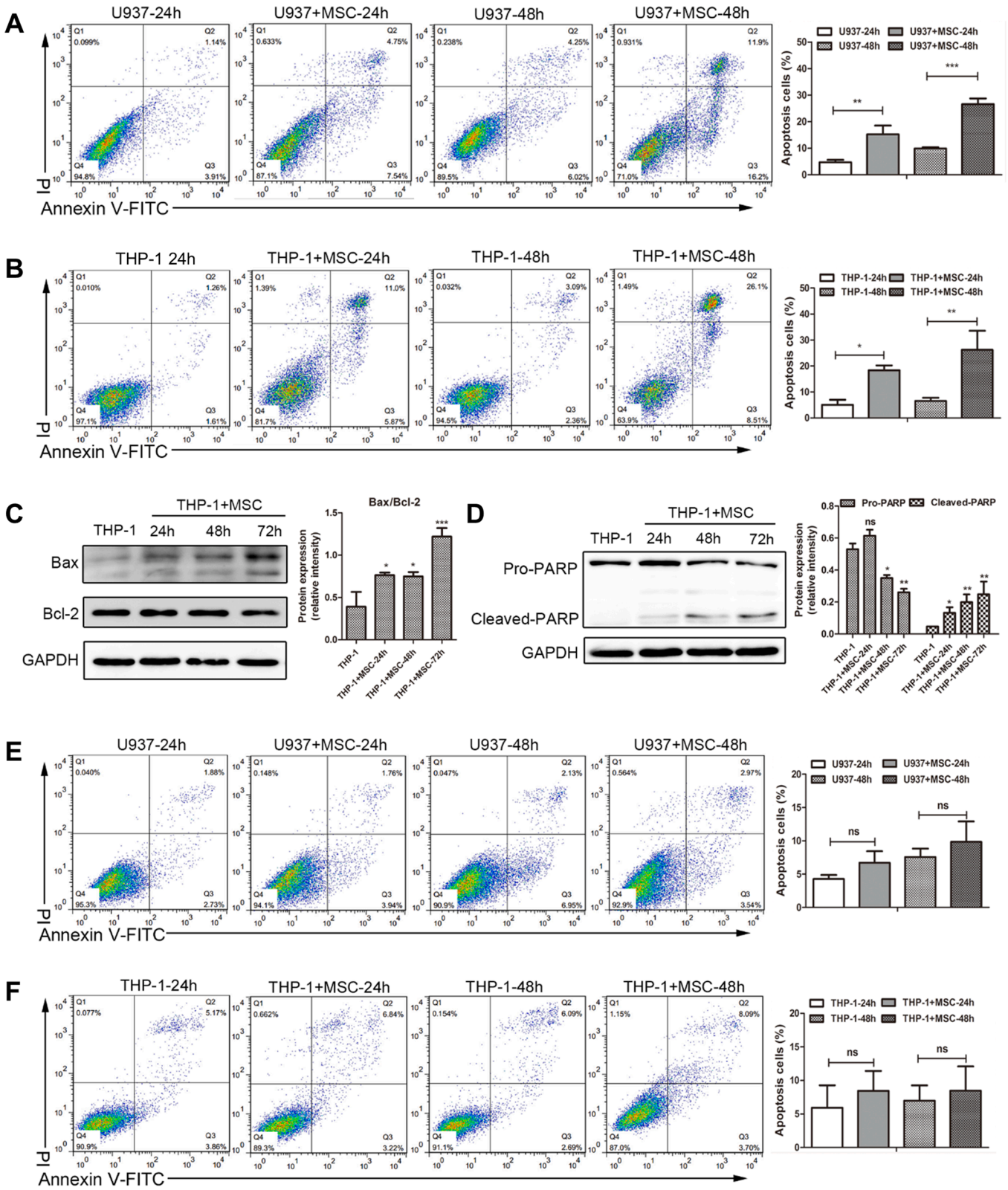

Fig. 2. MSC promote the apoptosis of acute myeloid leukemia cells. (A) Flow cytometry for U937 cells with or without UC-MSCs co-culture at 24 or 48 h (left). The apoptotic fractions were quantified on the right. (B) Flow cytometry for THP-1 cells with or without UC-MSCs co-culture at 24 or 48 h (left). The apoptotic fractions were quantified on the right. (C) Western blotting for Bax, Bcl-2 in THP-1 cells with or without UC-MSCs co-culture, the Bax to Bcl-2 ratio was determined on the right panel. (D) Western blotting for the expression of Pro-PARP and cleaved-PARP in THP-1 cells with or without UC-MSCs co-culture. Data were quantified on the right. (E-F) U937 (E) and THP-1 cells (F) were cultured alone or co-cultured in transwells with UC-MSCs for 24 or 48 h. The Annexin V/PI expression in AML cells was analyzed by flow cytometry. The apoptotic fractions of U937 and THP-1 cells were quantified on the right. Data are represented as the mean ± S.E.M. ($n = 3$; * $p < 0.05$; ** $p < 0.01$).

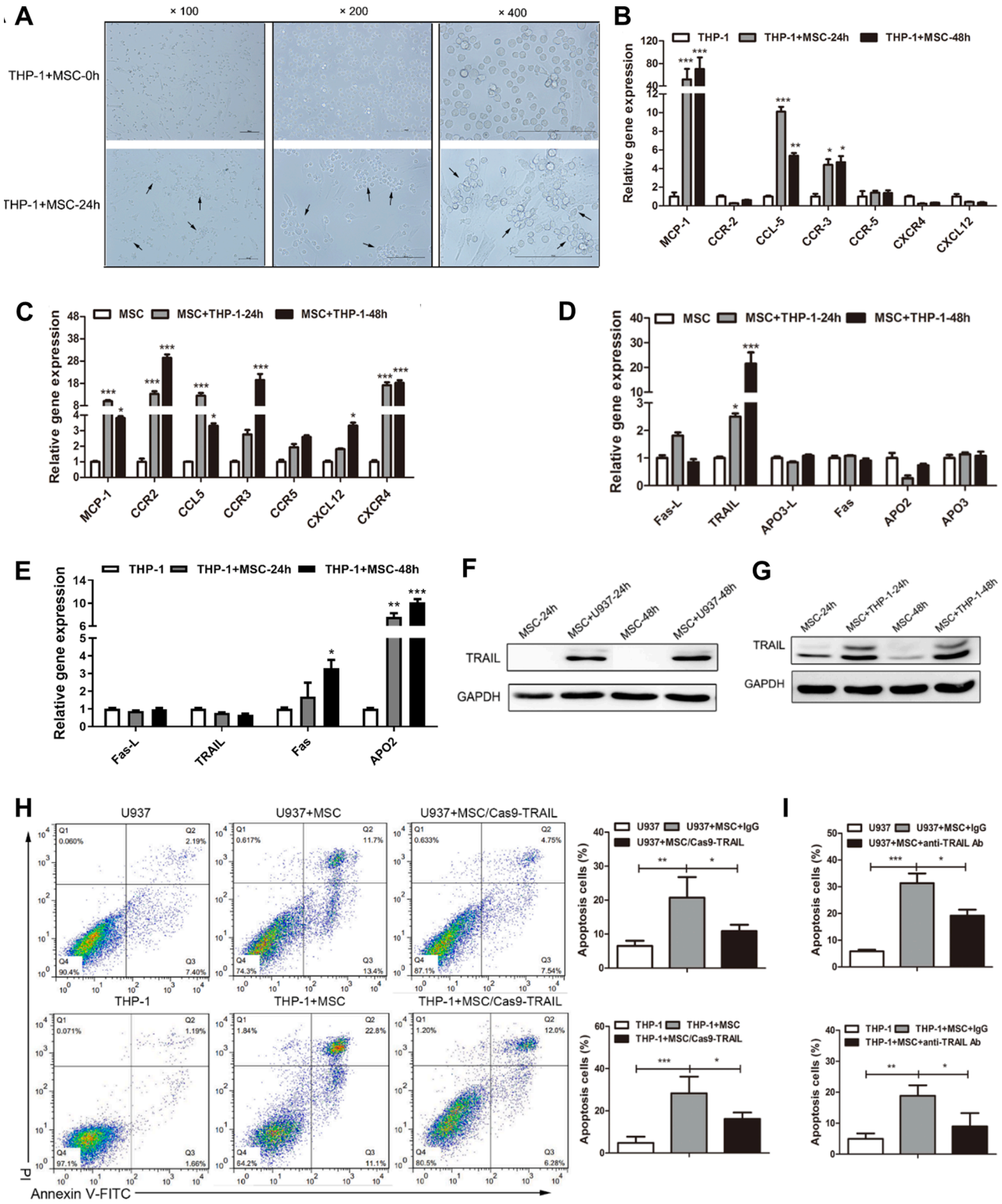

Fig. 3. Identification of TRAIL as the key effector in MSC-induced AML apoptosis. MSC were co-cultured with U937 or THP-1 cells for 24 or 48 h. (A) Representative optical microscope image; (B-C) The relative expression of the chemokines and chemokine receptors in THP-1 (B) and MSC (C) was assessed by RT-qPCR. (D) The relative gene expression of the chemokines and chemokine receptors Fas-L, TRAIL, Fas, APO3L, APO2 and APO3 in UC-MSCs with or without THP-1 co-culture was assessed by RT-qPCR. (E) The relative expression of the chemokines and chemokine receptors Fas-L, TRAIL, Fas, and APO2 in THP-1 with or without UC-MSCs coculture was assessed by RT-qPCR. (F-G) Western blotting for TRAIL in the MSC after incubating with U937 (F) and THP-1 cells (G) for 1 or 2 days. (H) Apoptosis of U937 (top) and THP-1 cells (bottom) was measured by flow cytometry. U937 and THP-1 cells were cultured alone or co-cultured with UC-MSCs in the presence or absence of a TRAIL blocking antibody for 48 h. The apoptotic percentages were quantified on the right. (I) U937 (top) and THP-1 cells (bottom) were cultured alone or co-cultured with TRAIL-knockout UC-MSCs for 48 h. The apoptotic percentages of U937 and THP-1 cells were analyzed by flow cytometry. Data are represented as the mean ± S.E.M. Statistical significance was determined by one-way ANOVA. **: $p < 0.01$, ***: $p < 0.001$ for triplicate experiments.

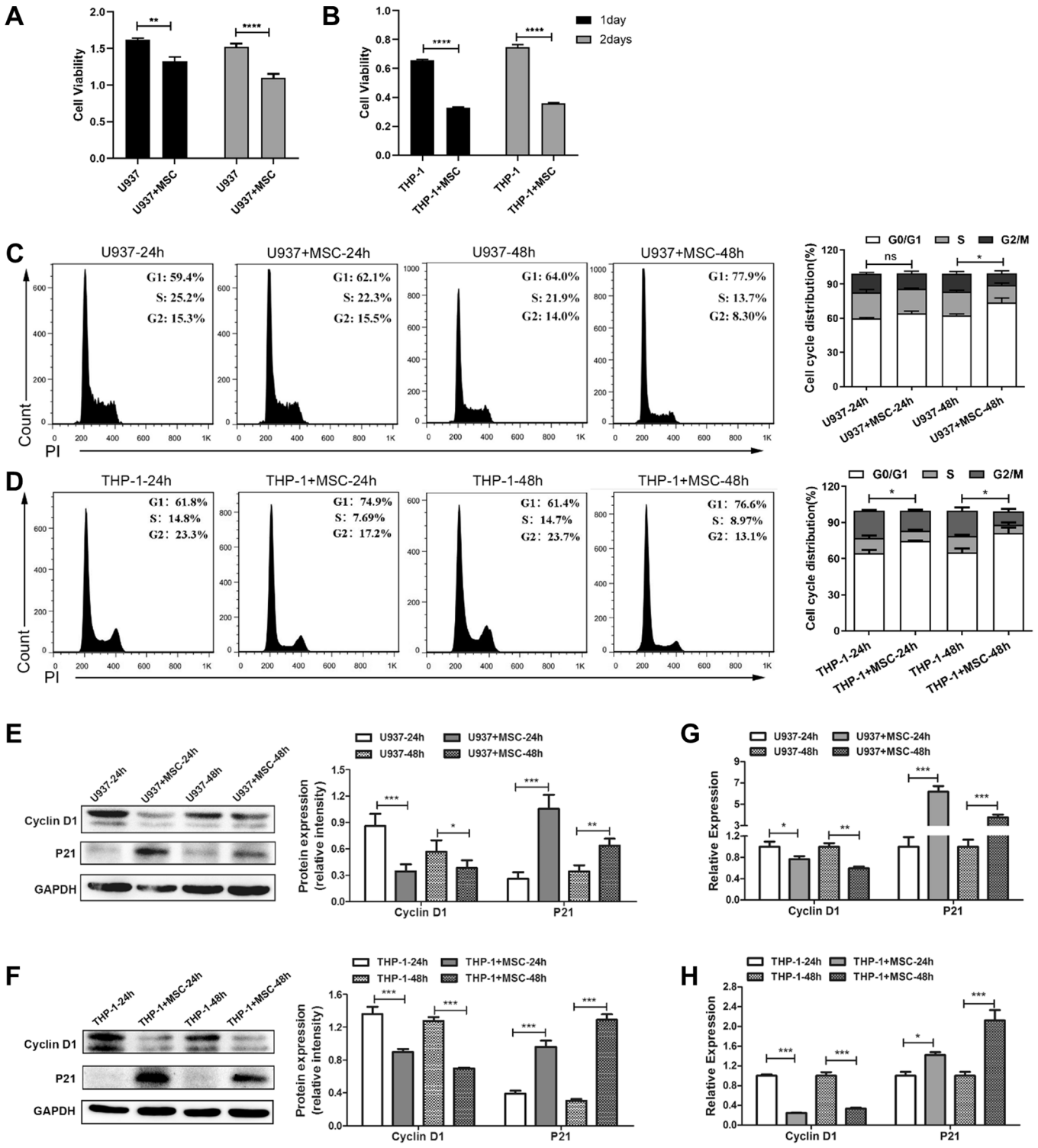

Fig. 4. UC-MSCs induce the G0/G1 cell cycle arrest in U937 and THP-1 cells. (A-B) After 1- or 2-days' incubation with UC-MSCs, the viability of U937 (A) and THP-1 (B) cells were detected by CCK8 assays. (C-D) MSC induce alterations of the cell cycle. U937 (C) and THP-1 (D) cells were treated with MSC for 1 or 2 days, and the cells were stained with propidium iodide and analyzed by flow cytometry. Results are representatives of three independent experiments. (E-F) Western blotting for the expression of cyclin D1, p21 in U937 (E) and THP-1 (F) cells upon the co-culture with or without MSC for 1 or 2 days. (G-H) Relative transcript expressions of cyclin D1 and p21 were decreased in U937 (G) and THP-1 (H) cells; the results were detected by RT-qPCR. Data are represented as the mean ± S.E.M. Statistical significance was determined by one-way ANOVA. **: $p < 0.01$, ***: $p < 0.001$ for triplicate experiments.

Cas9 was applied to generate TRAIL knockout MSC (MSC/Cas9-TRAIL). The flow cytometry data indicated that treatment with MSC/Cas9-TRAIL reduced apoptotic U937 cells from 20.7% to 10.9%, and reduced the apoptosis in THP-1 cells from 28.3 to 16.15% (Fig. 3I). Collectively, these data suggested that TRAIL is required for MSC-mediated AML cell apoptosis.

3.3. UC-MSCs inhibit AML cell proliferation and induce cell cycle arrest

Although there was no significant difference in apoptosis of AML cells in transwell co-culture system, a significant decrease in the cellular viability of in U937 and THP-1 cells was observed (Fig. 4A-B). Moreover, MSC treatment upregulated the G1 proportion of U937 and THP-1 cells (Fig. 4C-D), suggesting that MSC might induce cell cycle arrest through

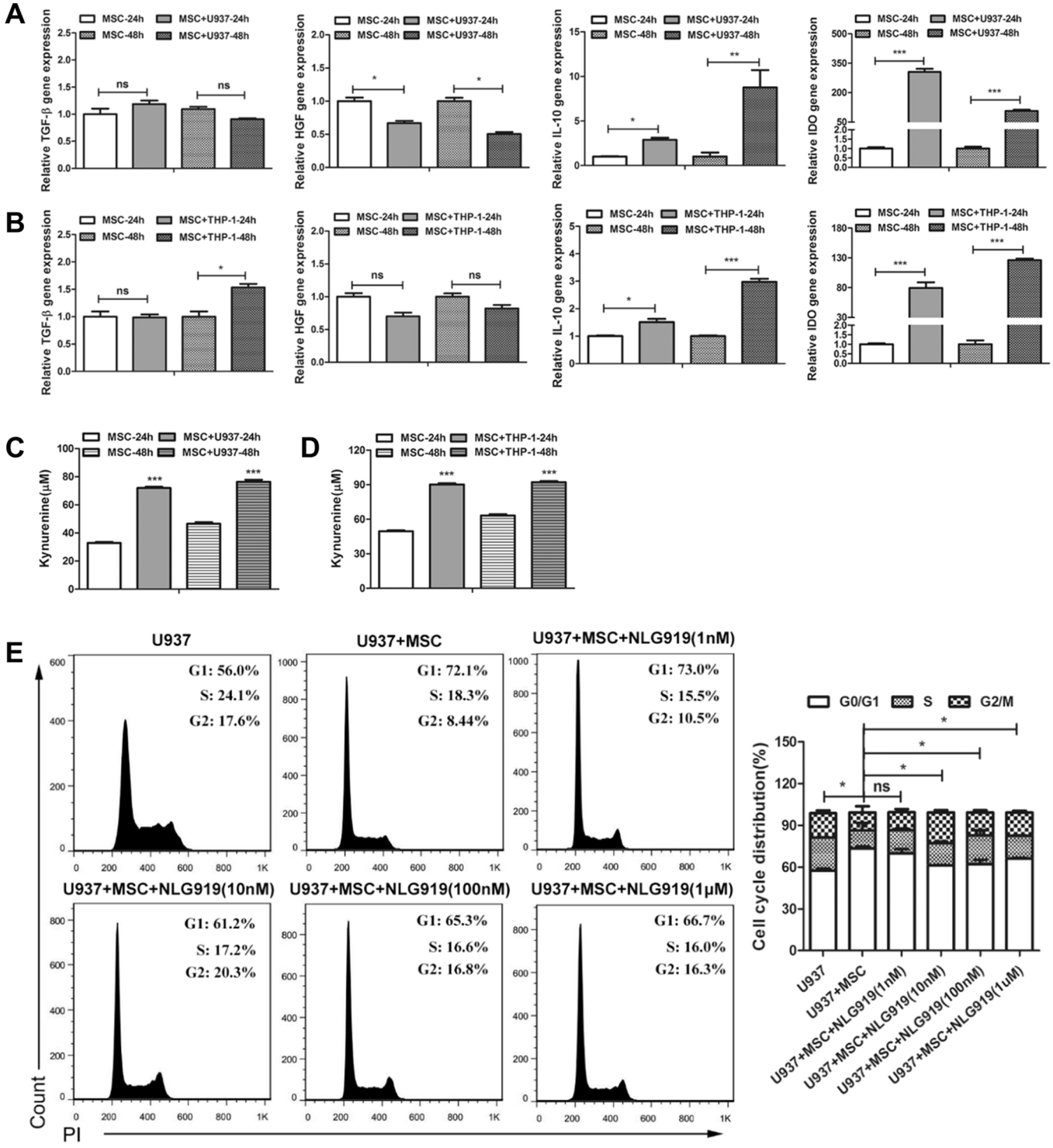

Fig. 5. IDO mediates the cell cycle arrest induced by UC-MSCs. (A-B) Relative gene expression of TGF-β, HGF, IL-10 and IDO were detected by RT-qPCR. (C-D) Kynurenine concentration in the conditioned medium of MSC treated with U937 (C) and THP-1 cells (D) was measured to detect the enzymatic activity of IDO. (E) The MSC-mediated cell cycle arrest in U937 cells were reversed by NLG919. Data are represented as the mean ± S.E.M. Statistical significance was determined by one-way ANOVA. **: $p < 0.01$, ***: $p < 0.001$ for triplicate experiments.

regulating G1-S checkpoint. U937 and THP-1 cells were incubated with MSC for 1 or 2 days, and the expression of G1/S checkpoint associated Cyclin D1 and Cyclin dependent kinase inhibitor p21 in U937 and THP-1 cells was examined. We found decreased Cyclin D1 and increased p21 expression in MSC-treated U937 and THP-1 cells (Fig. 4E-F). The Cyclin D1 and p21 transcripts were also downregulated or upregulated, respectively (Fig. 4G-H). Taken together, these results showed that MSC inhibited the viability and blocked the cell cycle progression of AML cells.

3.4. IDO from MSC blocks the cell cycle progression in AML cells

Many cytokines have been shown to be involved in MSC-mediated cell cycle arrest, such as TGF-β, hepatocyte growth factor (HGF) and indoleamine 2,3-dioxygenase (IDO) [30,31]. We then examined the expression of these soluble proteins in MSC in the absence or presence of U937 and THP-1 cells. Notably, we found that IDO showed the highest fold expression in presence of AML cells (Fig. 5A-B). Kynurenine, the metabolic product of tryptophan by IDO [32], was significantly upregulated in the supernatant from the co-incubated MSC (Fig. 5C-D), indicating that MSC were activated by AML cells and could induce massive IDO expression. To investigate the role of IDO in MSC-induced cell cycle inhibition, U937 and THP-1 cells were treated by MSC in the presence of NLG919, a potent IDO pathway inhibitor [33], the cell cycle distribution was then analyzed. The results showed that NLG919 significantly decreased the G1 fraction (Fig. 5E), indicating that the cell cycle arrest of AML cells induced by MSC was restored by blocking IDO activity. Collectively, these data showed that IDO is required for MSC-mediated cell cycle arrest.

3.5. TNF-α and IFN-γ priming strengthens the pro-apoptotic activity of MSC

Several previous studies have suggested that pro-inflammatory cytokines, such as IFN-γ and TNF-α can induce IDO and TRAIL expression in MSC. Therefore, we first measured the expression of IFN-γ and TNF-α from human AML samples. We extracted data from The Cancer Genome Atlas (TCGA) and found that high expression of IFN-γ and TNF-α was found in AML cells compared with healthy cells (Fig. 6A). To further confirm IFN-γ and TNF-α secretion by AML cells in co-culture, U937 and THP-1 cells were incubated with MSC for 1 or 2 days and then separately cultured for 2 days. RT-qPCR and ELISA were performed to compare

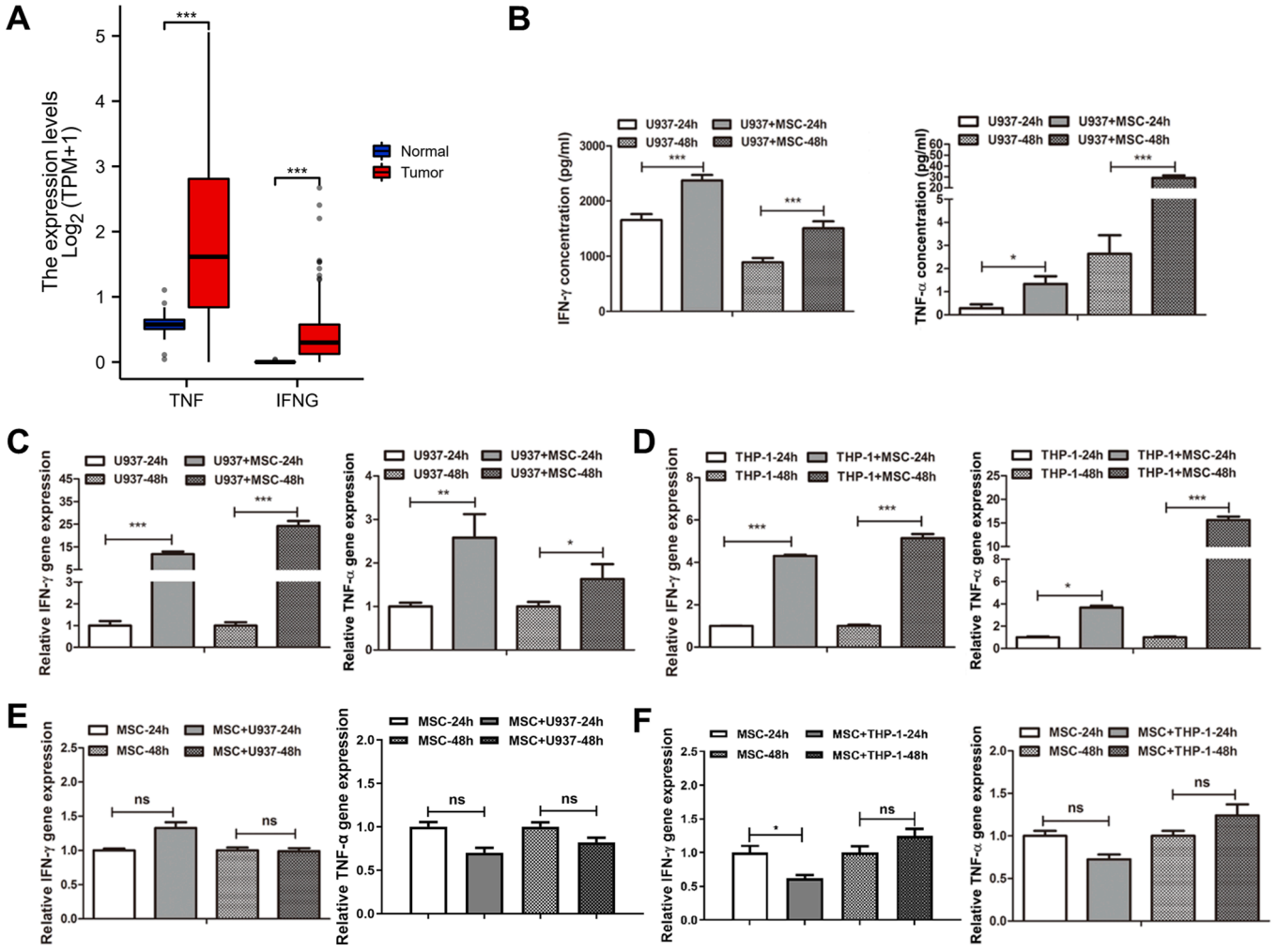

Fig. 6. MSC induce U937 and THP-1 cells to express inflammatory factors TNF-α and IFN-γ. (A) Differential expression analysis of RNA-seq data from AML patients and normal samples. A plot showing TNF-α (left) and IFN-γ (right) gene expression in 70 Normal samples (blue) as compared to 173 samples of AML patients (red) from the Genotype-Tissue Expression (GTEx) project and The Cancer Genome Atlas (TCGA). (B) Secreted IFN-γ and TNF-α from U937 cells following UC-MSCs treatment were measured by ELISA. (C-D) Relative gene expressions of IFN-γ and TNF-α in U937 (C) and THP-1 (D) cells with or without UC-MSCs co-culture. (E-F) Relative gene expressions of IFN-γ and TNF-α in UC-MSCs with or without U937 (E) or THP-1 cells (F) stimulation. The results were detected by RT-qPCR. Data are represented as the mean ± S.E.M. Statistical significance was determined by one-way ANOVA. **: $p < 0.01$, ***: $p < 0.001$ for triplicate experiments. (For interpretation of the references to colour in this figure legend, the reader is referred to the web version of this article.)

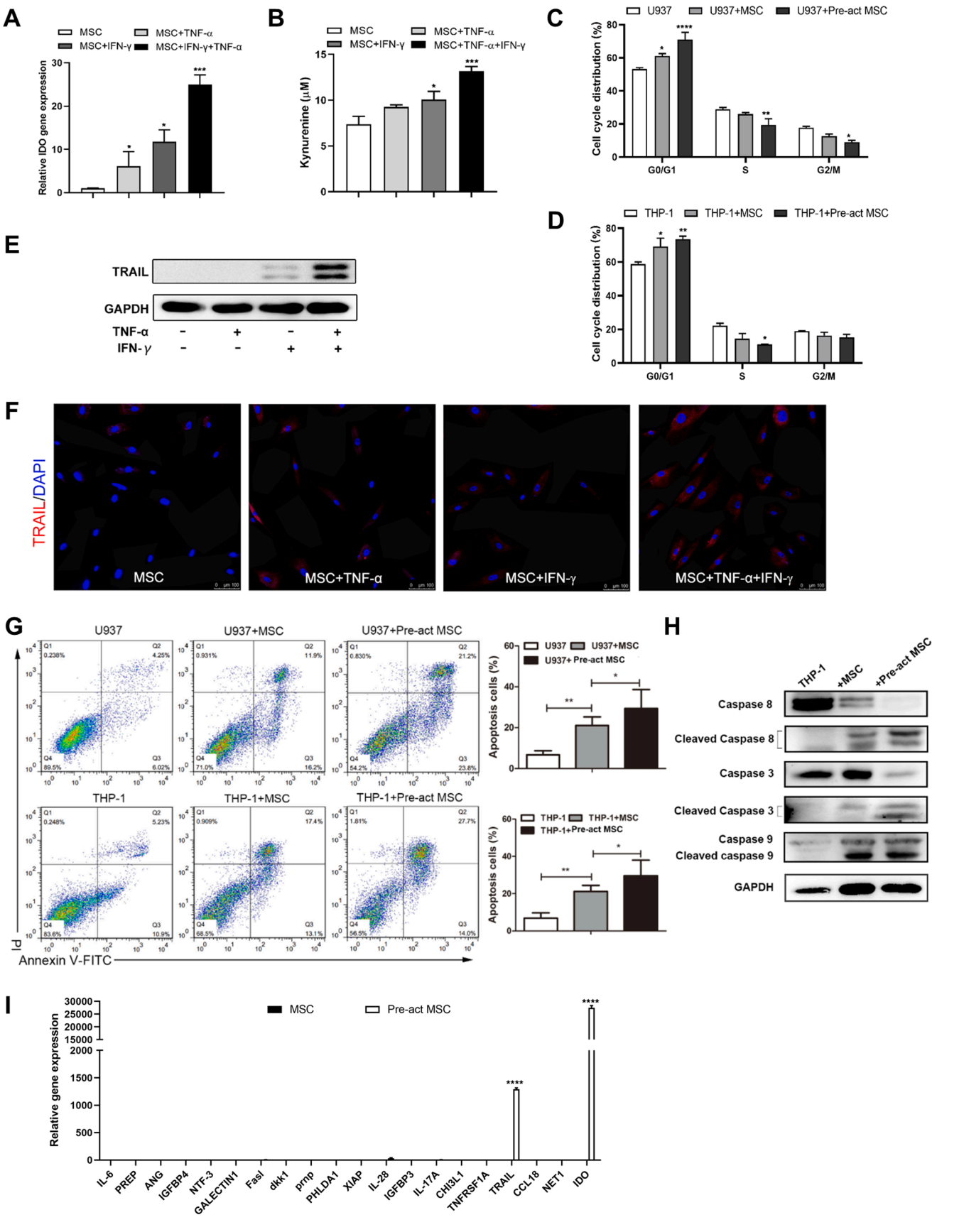

(caption on next page)

Fig. 7. TNF-α and IFN-γ enhances the anti-leukemia activity of UC-MSCs. (A) Relative gene expression of IDO in MSC in the presence of TNF-α or IFN-γ alone or in combination. (B) The enzymatic activity of IDO was detected by measuring the Kynurenine concentration of MSCs conditioned medium. (C-D) The percentage of U937 (C) and THP-1 (D) cells in G0/G1, S, G2/M phase was assayed by FACS after incubating with MSC or Pre-act MSC. (E) Western blot for TRAIL in UC-MSCs in the presence of TNF-α and/or IFN-γ. (F) MSC were treated with TNF-α and/or IFN-γ for 24 h. The expression of TRAIL was analyzed by immunofluorescence microscopy. TRAIL was labeled with anti-TRAIL (red). Nuclei were labeled with DAPI (blue). Scale bars, 100 μm. (G) The apoptosis of U937 (upper) and THP-1 cells (lower) were measured by flow cytometry, the graphic shows the apoptotic percentages of U937 and THP-1 cells. (H) THP-1 cells were treated with MSC or Pre-act MSC for 48 h. Lysates were subjected to immunoblotting for the detection of caspase-3, -8, -9 in THP-1 cells. (I) The mRNA levels of the differentially expressed proteins were measured by quantitative real-time PCR. Data are represented as the mean ± S.E.M. Statistical significance was determined by one-way ANOVA. $*p < 0.05$, $**p < 0.01$, or $***p < 0.001$ for 3 independent experiments. (For interpretation of the references to colour in this figure legend, the reader is referred to the web version of this article.)

IFN-γ and TNF-α expressions in U937 cells and MSC. The expression of IFN-γ and TNF-α was significantly elevated in U937 and THP-1 cells when they were co-cultured with MSC (Fig. 6B-D), whereas no significant changes in IFN-γ and TNF-α expression were found in MSC with or without U937/THP-1 co-culture (Fig. 6E-F), indicating that IFN-γ and TNF-α were secreted by AML cells.

To confirm whether IFN-γ and TNF-α can induce MSC activation, MSC were treated with IFN-γ (50 ng/ml) or TNF-α (20 ng/ml) alone or in combination. As shown in Fig 7A, a massive amount of IDO expression was observed in MSC following IFN-γ and TNF-α priming. Consistently, kynurenine level was also elevated when MSC were co-treated with IFN-γ and TNF-α (Fig. 7B). Furthermore, IFN-γ and TNF-α pre-treated MSC (Pre-act MSC) also reduced cell proliferation, resulting in the accumulation of AML cells in the G0/G1 phase (Fig. 7C-D). These data suggested that IFN-γ and TNF-α secreted by AML cells can induce IDO expression from MSC and strengthen the inhibitory effect on AML cell cycle progression.

We speculated that combinatorial treatment of TNF-α and IFN-γ may augment the pro-apoptotic effect of MSC on AML cells by increasing TRAIL expression. To test this hypothesis, the expression of TRAIL in MSC following IFN-γ and TNF-α stimulation (Pre-act MSC) was first measured. We found that combined administration of IFN-γ and TNF-α remarkably stimulated the expression of TRAIL (Fig. 7E). In addition, increased expression of TRAIL was observed in Pre-act MSC (Fig. 7F). Subsequently, we assessed the effect of Pre-act MSC on AML cell apoptosis. Flow cytometry analysis revealed a significantly increase in apoptotic fractions of U937 and THP-1 cells with Pre-act MSC treatment (Fig. 7G). Consistently, the activation of caspase-3, -8 and caspase-9 were also observed in MSC/Pre-MSC-treated THP-1 cells. The cleaved caspase-3, -8 and cleaved caspase-9 were significantly increased (Fig. 7H), suggesting that MSC induced AML cell apoptosis through activating caspase pathways in AML cells. It is reported that the strong paracrine capacity of MSC is the main mechanism of immunomodulatory and anti-tumor functions of MSC. To investigate whether there are other molecules secreted by MSC contribute to the pro-apoptosis effect of MSC on AML cells, we compared the differential expressed genes (DEGs) rigidly and clustered the apoptosis-related proteins between bone marrow-derived MSC (BMMSC) and BMMSC stimulated with TNF-α and IFN-γ (GSE142816), and screened the anti-tumor proteins secreted by MSC[34,35]. As a result, a total of 20 proteins (including TRAIL and IDO) were considered to induce AML apoptosis probably. Then, quantitative RT-PCR (qRT-PCR) was used to evaluated the expression of these protein. Among these candidates, IDO and TRAIL exhibited the highest induction levels (>27000-fold and 1200-fold) of gene expression, indicating that IDO and TRAIL play the key role of MSC-mediated AML cell apoptosis (Fig. 7I). Taken together, these results suggested that IFN-γ and TNF-α may enhance the expression of IDO and TRAIL and amplify the proapoptotic activity in MSC.

3.6. Pretreated MSC attenuates leukemia cell burden and prolongs the survival of AML mice

To determine the anti-leukemia function of pretreated MSC, AML mice were treated with MSC or Pre-act MSC and cytarabine was used as a positive control (Fig. 8A). Twenty-one days post injection, mice in MSC and Pre-act MSC treated groups showed improved survival. The median survival was 22 days in MSC-treated group, 30 days in Pre-act MSC-treated group, 23 days in cytarabine-treated group and 19 days in the saline-treated group (Fig. 8B). In addition, treatment with MSC, pre-act MSC or cytarabine substantially reduced the leukemia burden in both peripheral blood (PB) and bone marrow (BM) compared to that in saline-treated mice (Fig. 8C-D). Notably, the leukemia burden of the Pre-act MSC-treated mice decreased to 9% in PB and 1% in BM. Furthermore, a significant attenuation of splenic infiltration was shown in Pre-act MSC-treated mice (Fig. 8E). A remarkable recession of hepatosplenomegaly could also be observed in Pre-act MSC-treated mice compared with those in saline-treated mice (Fig. 8F-G). These findings suggested that MSC treatment indeed showed an anti-leukemia function in the mouse AML model and provided *in vivo* evidence that administration of IFN-γ and TNF-α in pretreated MSC could increase the therapeutic efficacy in AML.

3.7. Pre-act MSC induce apoptosis of cells from patients with myelomonocytic and monocytic AML

Then we collected peripheral blood samples from 13 myelomonocytic and monocytic AML patients and measured apoptosis in AML cells after 48 h incubation with MSC. As shown in Fig. 9A and 9B, MSC significantly induced apoptosis of AML cells from 5 patients (AML#1, #3, #4, #5, #12), meanwhile incubation of AML primary cells with Pre-act MSC also resulted in increased apoptosis (seven out of 13), demonstrating the efficacy of MSC in AML patients. In summary, our data suggested an efficient pretreatment method to increase the pro-apoptotic ability of MSC and provided a promising alternative therapy for AML.

3.8. MSC do not cause cytotoxic and acute toxic effect

To evaluate the potential toxicity of MSC, peripheral blood mononuclear cells (PBMCs) from healthy donors were cultured in the presence or absence of MSC/Pre-act MSC for 6, 12, 24 or 48 h, and apoptosis was evaluated by annexin V/PI double staining. Flow cytometry analysis showed that MSC not only did not induce apoptosis of PBMCs, but also improved PBMCs survival surprisingly (Fig. 10A). Moreover, the acute toxicity of MSC was monitored in adult male C57BL/6 mice after a single intravenous injection. The control group was given 100 μl of physiological saline per animal, and the treatment group received the same volume of a suspension containing MSC (10^8 kg^{-1}). The animals were euthanized 7 days after the administration. Normal hematological parameters and blood biochemical indexes were detected and no statistical significance was observed in MSC-treated group in comparison with the control group (Fig. 10B). Moreover, the histopathological analysis of the heart, lung, liver, spleen, kidney revealed that MSC administration did not induce clear pathological alterations (Fig. 10C). These parameters suggested that MSC administration showed no MSC-related toxicity, consistent with other investigations which highlighted that MSC therapy was safe and well tolerated [36,37]. Taken together, there is no evidence of a link between MSC and acute infusional toxicity, organ system complications, infection or death.

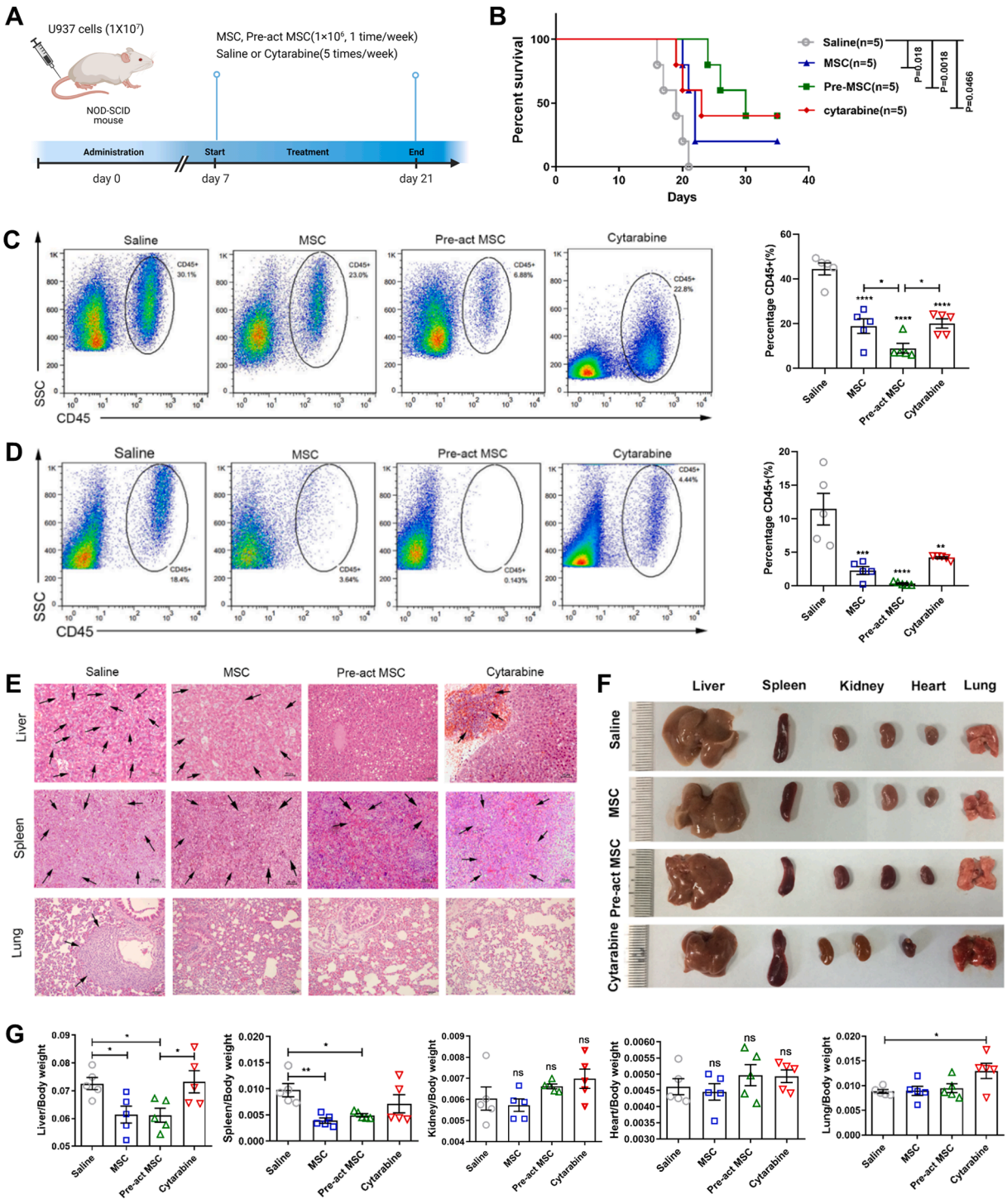

Fig. 8. Pretreatment with UC-MSCs prolonged survival and attenuated leukemic cells burden in an AML mouse model. (A) Schematic of the experimental design used for (B-E). (B) Survival curves of AML recipients treated with MSC, Pre-act MSC, cytarabine or vehicle until sacrificed. (C) Leukemic cells in peripheral blood of vehicle, MSC, Pre-act MSC and cytarabine treated mice during AML progression after 30 days of transplantation ($n = 5$), the percentages of hCD45-positive cells in peripheral blood were quantified on the right. (D) Leukemic cells in peripheral blood of vehicle, MSC, Pre-act MSC or cytarabine treated mice during AML progression after 30 days of transplantation ($n = 5$), the percentages of CD45-positive cells in in bone marrow were shown on the right. (E) Representative histological images (H&E staining) of hepatic, splenic and pulmonic infiltration from AML mice. (F) Visceral organs (liver, spleen, kidney, heart and lung) isolated from AML mice treated with MSC, Pre-act MSC or cytarabine. (G) The ratio of organ to body weight of mice as described in (F). All statistical data in this figure are presented as mean ± SEM. One-way ANOVA and Tukey's multiple comparisons test are shown. ns. Nonsignificant $p > 0.05$, * $p < 0.05$, ** $p < 0.01$, *** $p < 0.001$, **** $p < 0.0001$.

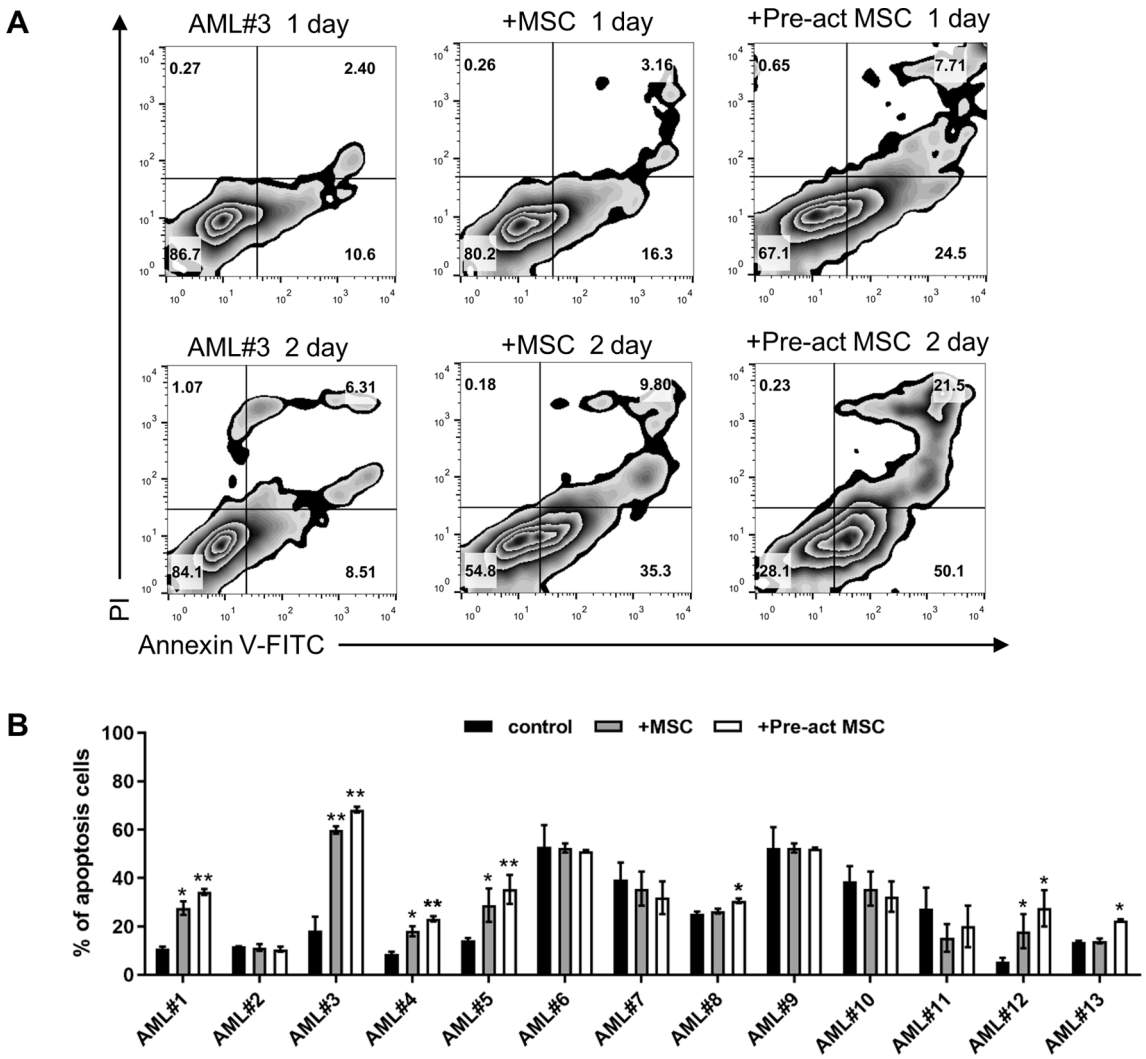

Fig. 9. Pre-act MSCs induce apoptosis of primary AML cells. (A) Primary AML cells were cultured with Pre-act MSCs for 24 or 48 h. Apoptosis in primary AML cells was assessed by annexin V/PI binding and analyzed by flow cytometry. (B) Apoptotic primary human cells from AML patients after MSCs or Pre-act MSC incubation.

4. Discussion

Despite increased understanding of AML pathogenesis, conventional treatment has not changed significantly in the past decades. Allogeneic HSCT following cytotoxic chemotherapy is commonly applied to treat AML patients. However, adverse effects often occur in AML patients after chemotherapy, and relapse has become a major obstacle following HSCT. Approximately 40% of post-HSCT AML patients will relapse[11,38]. Following the success of CAR-T cell therapy in ALL and B-cell lymphoma, substantial efforts have been done to translate this approach for AML treatment. Unlike B cell malignancies with extensive expression of antigens such as CD19, CD20, CD22, or BCMA [39], most targeted tumor antigens in myeloid malignancies are shared with healthy myeloid cells including HSPCs, resulting in prolonged myeloablation following CAR-T [40,41]. Furthermore, the clinical outcome of AML patients remains suboptimal, prompting a need for alternative therapeutic approaches. In this study, we demonstrated that UC-MSCs induced TRAIL-mediated apoptosis and arrest the cell cycle progression in AML cells by secreting IDO. Moreover, incubation with IFN-γ and TNF-α further inspired MSCs to produce more TRAIL and IDO, and pre-activated MSCs enhanced apoptosis in primary AML cells and reduced the tumor load in a xenograft mouse model. The anti-leukemic activity of the pre-activated MSCs may provide a promising alternative for AML treatment.

MSCs are broadly used for therapeutic purposes to treat malignant diseases. Over 1300 MSCs clinical trials have been registered on ClinicalTrials.gov. Application of MSCs depends on its "tumor-homing" and immunomodulatory properties. Compared to bone marrow-derived MSCs (BM-MSCs) and adipose-derived MSCs, UC-MSCs present many advantages. First, the collection of UC-MSCs is non-invasive and harmless, with minimal ethical issues, whereas adult tissue-derived MSCs require invasive procedures with pain and potential infections. Second, UC-MSCs display a higher proliferation capacity and genetic stability, as no remarkable alterations are observed in a long-term culture *in vitro* [42,43]. Importantly, increasing evidence has shown that UC-MSCs can play an anti-tumor function by inhibiting the proliferation or inducing the apoptosis of tumor cells with neglectable side effects reporting [36,44–46]. Similarly, our results have manifested that UC-MSCs can induce apoptosis in both primary AML cells and AML cell lines by upregulating TRAIL expression. In addition, we have also found that IDO secreted by UC-MSCs can arrest the cell cycle at the G0/G1 phase in AML cells, with increased expression of cyclin D1 and decreased expression of p21. These data imply that UC-MSCs have the potential to restrain AML progression.

It has been shown that IFN-γ and TNF-α have synergistic anti-tumor effects by augmenting TRAIL-induced apoptosis in cancer cells [47-49]. In current work, we noted high expression of IFN-γ and TNF-α in

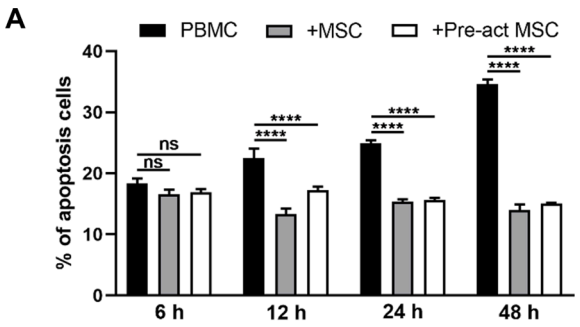

B

Parameter	control	MSC
ALT（U.l/L）	30.18±2.49	32.24±2.27
AST（U.l/L）	98.10±20.36	127.10±18.61
BUN（M.l/L）	8.80±0.330	8.668±0.56
CRE（U.l/L）	18.25±1.35	19.2±0.80
T-BIL（U.l/L）	0.925±0.16	1.04±0.07
TP （g / L）	51.38±0.56	51.46±1.07

C

Parameter	control	MSC
WBC ($\times 10^9$/μL)	2.18±0.17	1.60±0.28
RBC ($\times 10^{12}$/μL)	8.98±0.12	8.02±1.85
Lymphocytes(%)	79.18±4.78	83.25±1.99
Eosinophils (%)	1.00±0.17	0.95±0.18
Basophils (%)	0.35±0.12	0.30±0.07
Platelets($\times 10^{11}$/μL)	9.94±0.69	12.14±0.11
MCV(fL)	43.63±0.17	43.25±0.36
MCHC(%)	339.5±4.62	336.0±4.04

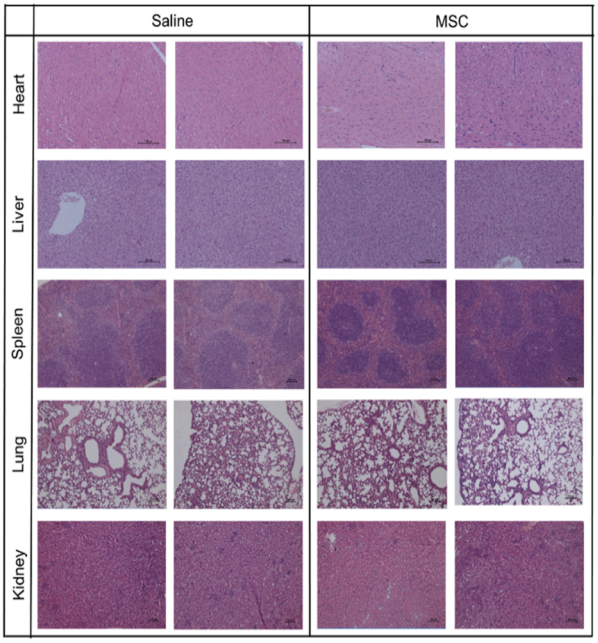

Fig. 10. Evaluation of acute toxicity and cytotoxicity Effect of MSC. (A) PBMC were cultured with MSC or Pre-act MSCs for the indicated periods of time. Apoptosis in PBMC was assessed by annexin V/PI binding and analyzed by flow cytometry. (B-C) Effects of MSC treatment on blood biochemical indexes (B) and hematological parameters (C). ALT: alanine transaminase. AST: aspartate aminotransferase. BUN: urea nitrogen. Crea: creatinine. T-BIL: total bilirubin. Tp: total serum protein. WBC: white blood cell. RBC: red blood cell. MCV: mean corpuscular volume. MCHC: mean corpuscular hemoglobin concentration. (D) Representative histopathological analysis of heart, liver, spleen, lung and kidney from mice after treatment with MSC or Saline for 7 days. Magnification 10× and scale bar = 100 μm. N = 4–5 per group. All statistical data in this figure are presented as mean ± SEM. One-way ANOVA and Tukey's multiple comparisons test are shown. ns. Nonsignificant $p > 0.05$, * $p < 0.05$, ** $p < 0.01$, *** $p < 0.001$, **** $p < 0.0001$. (For interpretation of the references to colour in this figure legend, the reader is referred to the web version of this article.)

myelomonocytic and monocytic AML patients, consistent with ELISA data that AML cells secreted IFN-γ and TNF-α to further enhance the production in the presence of UC-MSCs. Since pre-conditioning MSCs with IFN-γ and TNF-α showed immunosuppressive function in type 2 diabetes [50], multiple pre-activated regents have been investigated. Each cytokine can convert MSCs into a distinct functional state depending on the dose and duration [51-53]. Thus, we sought to determine whether pre-treatment of TNF-α (50 ng/ml) and IFN-γ (20 ng/ml) may augment the pro-apoptotic effect of MSCs. Here, we demonstrated that pre-treatment with TNF-α and IFN-γ in UC-MSCs upregulated the expression of TRAIL and strengthened the proapoptotic activities in AML cells. TRAIL has been considered as a promising anti-cancer agent, owing to its ability to induce apoptosis in tumor cells but not normal cells [54-56]. Moreover, we demonstrated that IDO expressed by UC-MSCs blocked cell-cycle progression in AML cells. In the co-culture system, we observed decreased cyclin D1 and increased p21 expression which correlated with enhanced cell cycle arrest. The anti-proliferative effect is attenuated by inhibiting IDO production, suggesting that IDO expression by UC-MSCs may induce cell-cycle arrest in AML cells. Not surprisingly, pre-treatment of UC-MSCs reinforced cell cycle arrest through upregulating IDO expression.

Contributing to the inherent tropism capacity of MSCs to migrate

toward lesion sites, MSCs are considered as an appropriate cytotherapeutic-based vehicle which can deliver cytokines, cytotoxic agents, prodrug-converting enzymes, immunostimulatory and anti-angiogenic molecular to tumor sites[57-59]. MSCs have been employed in several preclinical cancer models, which utilized their intrinsic anti-tumor properties or as a delivery vehicle [60-62]. For instance, genetically engineered IL-2-expressing MSCs could induce ovarian cancer cells apoptosis [63].Yu et al. showed that MSCs engineered to express a secreted form of TRAIL in combination with the low doses of 5-fluorouracil executed a synergistic pro-apoptotic effect in the colon cancer model[64]. These studies indicate that MSCs are the valuable anti-cancer vector that possesses the potential to be used to treat a number of different cancer types[65]. In our study, MSCs could deliver IDO and TRAIL to AML cells to promote cell apoptosis. Furthermore, pretreatment of MSCs amplifies the MSC-mediated pro-apoptotic effect by increasing delivery capacity to AML cells. Taken together, our findings demonstrated that MSC application as delivery vehicles hold great promise for the treatment of AML and the other cancers.

In summary, our data have demonstrated that UC-MSCs can promote apoptosis in AML cells implying that UC-MSCs may function as a therapeutic agent for treating AML. Importantly, IFN-γ and TNF-α pre-treatment can induce the production of TRAIL and IDO in UC-MSCs. The effects of pre-treatment are durable, since AML cells can also secrete high levels of IFN-γ and TNF-α. Furthermore, MSCs pre-treatment with cytokines such as IFN-γ and TNF-α can lower the risk of genetic mutations by random transfection with the *TRAIL* and *IDO* genes. Collectively, our findings provide an efficient therapeutic strategy that ameliorated the AML burden by treatment with pre-activated UC-MSCs.

CRediT authorship contribution statement

Luchen Sun: Methodology, Investigation, Data curation, Writing – original draft. **Jingyue Wang:** Data curation, Formal analysis. **Qiuping Wang:** Methodology, Formal analysis. **Zhonglei He:** Data curation. **Tingzhe Sun:** Validation, Writing – original draft. **Yongfang Yao:** Methodology, Data curation. **Wenxin Wang:** Methodology. **Pingping Shen:** Supervision, Writing – review & editing, Validation, Funding acquisition.

Declaration of Competing Interest

The authors declare that they have no known competing financial interests or personal relationships that could have appeared to influence the work reported in this paper.

Acknowledgments

Thanks to members of Shen's laboratory for helpful discussions, technical assistance, and critical reading of the manuscript.

This work was supported by grants from Guangdong Basic and Applied Basic Research Foundation (2021B1515120016); National Key Research and Development Program of China (2017YFA0506000); the Key Research and Development Program of Jiangsu Province, China-Social Development Projects (BE2020687).

References

[1] D.B. Sykes, Y.S. Kfoury, F.E. Mercier, M.J. Wawer, J.M. Law, M.K. Haynes, T. A. Lewis, A. Schajnovitz, E. Jain, D. Lee, H. Meyer, K.A. Pierce, N.J. Tolliday, A. Waller, S.J. Ferrara, A.L. Eheim, D. Stoeckigt, K.L. Maxcy, J.M. Cobert, J. Bachand, B.A. Szekely, S. Mukherjee, L.A. Sklar, J.D. Kotz, C.B. Clish, R. I. Sadreyev, P.A. Clemons, A. Janzer, S.L. Schreiber, D.T. Scadden, Inhibition of Dihydroorotate Dehydrogenase Overcomes Differentiation Blockade in Acute Myeloid Leukemia, Cell 167 (1) (2016) 171–186.e15.

[2] M. Greaves, Leukaemia 'firsts' in cancer research and treatment, Nat. Rev. Cancer 16 (3) (2016) 163–172.

[3] J. Murakami, Y. Shimizu, Hepatic manifestations in hematological disorders, Int. J. Hepatol. 2013 (2013), 484903.

[4] A. Lahoti, H. Kantarjian, A.K. Salahudeen, F. Ravandi, J.E. Cortes, S. Faderl, S. O'Brien, W. Wierda, G.N. Mattiuzzi, Predictors and outcome of acute kidney injury in patients with acute myelogenous leukemia or high-risk myelodysplastic syndrome, Cancer 116 (17) (2010) 4063–4068.

[5] J.M. Bennett, A. Orazi, Diagnostic criteria to distinguish hypocellular acute myeloid leukemia from hypocellular myelodysplastic syndromes and aplastic anemia: recommendations for a standardized approach, Haematologica 94 (2) (2009) 264–268.

[6] I. Henig, T. Zuckerman, Hematopoietic stem cell transplantation-50 years of evolution and future perspectives, Rambam Maimonides Med. J. 5 (4) (2014) e0028, https://doi.org/10.5041/RMMJ.2076917210.5041/RMMJ.10162.

[7] E. Estey, H. Döhner, Acute myeloid leukaemia, The Lancet 368 (9550) (2006) 1894–1907.

[8] J.V. Malfuson, A. Etienne, P. Turlure, T. de Revel, X. Thomas, N. Contentin, C. Terre, S. Rigaudeau, D. Bordessoule, N. Vey, C. Gardin, H. Dombret, A. Acute Leukemia French, Risk factors and decision criteria for intensive chemotherapy in older patients with acute myeloid leukemia, Haematologica 93 (12) (2008) 1806–1813.

[9] L. Crucitti, R. Crocchiolo, C. Toffalori, B. Mazzi, R. Greco, A. Signori, F. Sizzano, L. Chiesa, E. Zino, M.T. Lupo Stanghellini, A. Assanelli, M.G. Carrabba, S. Marktel, M. Marcatti, C. Bordignon, C. Corti, M. Bernardi, J. Peccatori, C. Bonini, K. Fleischhauer, F. Ciceri, L. Vago, Incidence, risk factors and clinical outcome of leukemia relapses with loss of the mismatched HLA after partially incompatible hematopoietic stem cell transplantation, Leukemia 29 (5) (2015) 1143–1152.

[10] J.M. Middeke, M. Fang, J.J. Cornelissen, B. Mohr, F.R. Appelbaum, M. Stadler, J. Sanz, H. Baurmann, G. Bug, K. Schafer-Eckart, U. Hegenbart, T. Bochtler, C. Rollig, F. Stolzel, R.B. Walter, G. Ehninger, M. Bornhauser, B. Lowenberg, J. Schetelig, Outcome of patients with abnl(17p) acute myeloid leukemia after allogeneic hematopoietic stem cell transplantation, Blood 123 (19) (2014) 2960–2967.

[11] P. Tsirigotis, M. Byrne, C. Schmid, F. Baron, F. Ciceri, J. Esteve, N.C. Gorin, S. Giebel, M. Mohty, B.N. Savani, A. Nagler, Relapse of AML after hematopoietic stem cell transplantation: methods of monitoring and preventive strategies. A review from the ALWP of the EBMT, Bone Marrow Transplant. 51 (11) (2016) 1431–1438.

[12] C. Rautenberg, U. Germing, R. Haas, G. Kobbe, T. Schroeder, Relapse of Acute Myeloid Leukemia after Allogeneic Stem Cell Transplantation: Prevention, Detection, and Treatment, Int. J. Mol. Sci. 20 (1) (2019).

[13] F.P. Tambaro, H. Singh, E. Jones, M. Rytting, K.M. Mahadeo, P. Thompson, N. Daver, C. DiNardo, T. Kadia, G. Garcia-Manero, T. Chan, R.R. Shah, W. G. Wierda, Autologous CD33-CAR-T cells for treatment of relapsed/refractory acute myelogenous leukemia, Leukemia 35 (11) (2021) 3282–3286.

[14] S. Mardiana, S. Gill, CAR T Cells for Acute Myeloid Leukemia: State of the Art and Future Directions, Front. Oncol. 10 (2020) 697.

[15] K.D. Cummins, S. Gill, Chimeric antigen receptor T-cell therapy for acute myeloid leukemia: how close to reality? Haematologica 104 (7) (2019) 1302–1308.

[16] S. Aravindhan, S.S. Ejam, M.H. Lafta, A. Markov, A.V. Yumashev, M. Ahmadi, Mesenchymal stem cells and cancer therapy: insights into targeting the tumour vasculature, Cancer Cell Int. 21 (1) (2021) 158.

[17] F. Zhang, J. Guo, Z. Zhang, Y. Qian, G. Wang, M. Duan, H. Zhao, Z. Yang, X. Jiang, Mesenchymal stem cell-derived exosome: A tumor regulator and carrier for targeted tumor therapy, Cancer Lett. 526 (2022) 29–40.

[18] L. Qiao, Z.-l. Xu, T.-J. Zhao, L.-H. Ye, X.-D. Zhang, Dkk-1 secreted by mesenchymal stem cells inhibits growth of breast cancer cells via depression of Wnt signalling, Cancer Lett. 269 (1) (2008) 67–77.

[19] R.H. Lee, N. Yoon, J.C. Reneau, D.J. Prockop, Preactivation of human MSCs with TNF-alpha enhances tumor-suppressive activity, Cell Stem. Cell 11 (6) (2012) 825–835.

[20] R. Liang, G.-S. Huang, Z. Wang, X.-Q. Chen, Q.-X. Bai, Y.-Q. Zhang, B.-X. Dong, W.-Q. Wang, Effects of human bone marrow stromal cell line (HFCL) on the proliferation, differentiation and apoptosis of acute myeloid leukemia cell lines U937, HL-60 and HL-60/VCR, Int. J. Hematol. 87 (2) (2008) 152–166.

[21] Y. Zhu, Z. Sun, Q. Han, L. Liao, J. Wang, C. Bian, J. Li, X. Yan, Y. Liu, C. Shao, R. C. Zhao, Human mesenchymal stem cells inhibit cancer cell proliferation by secreting DKK-1, Leukemia 23 (5) (2009) 925–933.

[22] M.W. Lee, S. Ryu, D.S. Kim, J.W. Lee, K.W. Sung, H.H. Koo, K.H. Yoo, Mesenchymal stem cells in suppression or progression of hematologic malignancy: current status and challenges, Leukemia 33 (3) (2019) 597–611.

[23] M. Krampera, L. Cosmi, R. Angeli, A. Pasini, F. Liotta, A. Andreini, V. Santarlasci, B. Mazzinghi, G. Pizzolo, F. Vinante, P. Romagnani, E. Maggi, S. Romagnani, F. Annunziato, Role for interferon-gamma in the immunomodulatory activity of human bone marrow mesenchymal stem cells, Stem Cells 24 (2) (2006) 386–398.

[24] N. Cheng, Y. Bei, Y. Song, W. Zhang, L. Xu, W. Zhang, N. Yang, X. Bai, Y. Shu, P. Shen, B7–H3 augments the pro-angiogenic function of tumor-associated

macrophages and acts as a novel adjuvant target for triple-negative breast cancer therapy, Biochem. Pharmacol. 183 (2021), 114298.
[25] M. Raisova, A.M. Hossini, J. Eberle, C. Riebeling, C.E. Orfanos, C.C. Geilen, T. Wieder, I. Sturm, P.T. Daniel, The Bax/Bcl-2 ratio determines the susceptibility of human melanoma cells to CD95/Fas-mediated apoptosis, J. Invest. Dermatol. 117 (2) (2001) 333–340.
[26] G. Del Poeta, A. Venditti, M.I. Del Principe, L. Maurillo, F. Buccisano, A. Tamburini, M.C. Cox, A. Franchi, A. Bruno, C. Mazzone, P. Panetta, G. Suppo, M. Masi, S. Amadori, Amount of spontaneous apoptosis detected by Bax/Bcl-2 ratio predicts outcome in acute myeloid leukemia (AML), Blood 101 (6) (2003) 2125–2131.
[27] F. Alcayaga-Miranda, J. Cuenca, P. Luz-Crawford, C. Aguila-Díaz, A. Fernandez, F. E. Figueroa, M. Khoury, Characterization of menstrual stem cells: angiogenic effect, migration and hematopoietic stem cell support in comparison with bone marrow mesenchymal stem cells, Stem Cell Res. Ther. 6 (2015) 32.
[28] J. Driscoll, T. Patel, The mesenchymal stem cell secretome as an acellular regenerative therapy for liver disease, J. Gastroenterol. 54 (9) (2019) 763–773.
[29] F. Belema-Bedada, S. Uchida, A. Martire, S. Kostin, T. Braun, Efficient homing of multipotent adult mesenchymal stem cells depends on FROUNT-mediated clustering of CCR2, Cell Stem Cell 2 (6) (2008) 566–575.
[30] M. Di Nicola, C. Carlo-Stella, M. Magni, M. Milanesi, P.D. Longoni, P. Matteucci, S. Grisanti, A.M. Gianni, Human bone marrow stromal cells suppress T-lymphocyte proliferation induced by cellular or nonspecific mitogenic stimuli, Blood 99 (10) (2002) 3838–3843.
[31] A.G. Laing, G. Fanelli, A. Ramirez-Valdez, R.I. Lechler, G. Lombardi, P.T. Sharpe, J. M. Hare, Mesenchymal stem cells inhibit T-cell function through conserved induction of cellular stress, PLoS ONE 14 (3) (2019) e0213170.
[32] A.A. Badawy, Kynurenine Pathway of Tryptophan Metabolism: Regulatory and Functional Aspects, Int. J. Tryptophan Res. 10 (2017), 1178646917691938.
[33] A. Nayak-Kapoor, Z. Hao, R. Sadek, R. Dobbins, L. Marshall, N.N. Vahanian, W. Jay Ramsey, E. Kennedy, M.R. Mautino, C.J. Link, R.S. Lin, S. Royer-Joo, X. Liang, L. Salphati, K.M. Morrissey, S. Mahrus, B. McCall, A. Pirzkall, D.H. Munn, J. E. Janik, S.N. Khleif, Phase Ia study of the indoleamine 2,3-dioxygenase 1 (IDO1) inhibitor navoximod (GDC-0919) in patients with recurrent advanced solid tumors, J. ImmunoTher. Cancer 6 (1) (2018) 61.
[34] J.J. McGuire, J.S. Frieling, C.H. Lo, T. Li, A. Muhammad, H.R. Lawrence, N. J. Lawrence, L.M. Cook, C.C. Lynch, Mesenchymal stem cell-derived interleukin-28 drives the selection of apoptosis resistant bone metastatic prostate cancer, Nat. Commun. 12 (1) (2021) 723.
[35] L. Cortes-Dericks, L. Froment, G. Kocher, R.A. Schmid, Human lung-derived mesenchymal stem cell-conditioned medium exerts in vitro antitumor effects in malignant pleural mesothelioma cell lines, Stem Cell Res. Ther. 7 (2016) 25.
[36] Y. Wang, H. Yi, Y. Song, The safety of MSC therapy over the past 15 years: a meta-analysis, Stem Cell Res. Ther. 12 (1) (2021) 545.
[37] L. Jin, X. Wang, Z. Qiao, Y. Deng, The safety and efficacy of mesenchymal stem cell therapy in diabetic lower extremity vascular disease: a meta-analysis and systematic review, Cytotherapy 24 (3) (2022) 225–234.
[38] A.J. Barrett, M. Battiwalla, Relapse after allogeneic stem cell transplantation, Expert Rev. Hematol. 3 (4) (2010) 429–441.
[39] U. Greenbaum, K.M. Mahadeo, P. Kebriaei, E.J. Shpall, N.Y. Saini, Chimeric Antigen Receptor T-Cells in B-Acute Lymphoblastic Leukemia: State of the Art and Future Directions, Front. Oncol. 10 (2020) 1594.
[40] B. De Moerloose, CAR-T treatment of pediatric AML: a long and winding road, Blood 137 (8) (2021) 1004–1006.
[41] S. Gill, S.K. Tasian, M. Ruella, O. Shestova, Y. Li, D.L. Porter, M. Carroll, G. Danet-Desnoyers, J. Scholler, S.A. Grupp, C.H. June, M. Kalos, Preclinical targeting of human acute myeloid leukemia and myeloablation using chimeric antigen receptor-modified T cells, Blood 123 (15) (2014) 2343–2354.
[42] A.K. Batsali, C. Pontikoglou, D. Koutroulakis, K.I. Pavlaki, A. Damianaki, I. Mavroudi, K. Alpantaki, E. Kouvidi, G. Kontakis, H.A. Papadaki, Differential expression of cell cycle and WNT pathway-related genes accounts for differences in the growth and differentiation potential of Wharton's jelly and bone marrow-derived mesenchymal stem cells, Stem Cell Res. Ther. 8 (1) (2017) 102.
[43] I. Christodoulou, F.N. Kolisis, D. Papaevangeliou, V. Zoumpourlis, Comparative Evaluation of Human Mesenchymal Stem Cells of Fetal (Wharton's Jelly) and Adult (Adipose Tissue) Origin during Prolonged In Vitro Expansion: Considerations for Cytotherapy, Stem Cells Int. 2013 (2013), 246134.
[44] Y. Yuan, C. Zhou, X. Chen, C. Tao, H. Cheng, X. Lu, Suppression of tumor cell proliferation and migration by human umbilical cord mesenchymal stem cells: A possible role for apoptosis and Wnt signaling, Oncol. Lett. 15 (6) (2018) 8536–8544.
[45] R. Ramasamy, E.W.F. Lam, I. Soeiro, V. Tisato, D. Bonnet, F. Dazzi, Mesenchymal stem cells inhibit proliferation and apoptosis of tumor cells: impact on in vivo tumor growth, Leukemia 21 (2) (2007) 304–310.
[46] M. Fonseka, R. Ramasamy, B.C. Tan, H.F. Seow, Human umbilical cord blood-derived mesenchymal stem cells (hUCB-MSC) inhibit the proliferation of K562 (human erythromyeloblastoid leukaemic cell line), Cell Biol. Int. 36 (9) (2012) 793–801.
[47] K. Suk, I. Chang, Y.H. Kim, S. Kim, J.Y. Kim, H. Kim, M.S. Lee, Interferon gamma (IFNgamma) and tumor necrosis factor alpha synergism in ME-180 cervical cancer cell apoptosis and necrosis. IFNgamma inhibits cytoprotective NF-kappa B through STAT1/IRF-1 pathways, J. Biol. Chem. 276 (16) (2001) 13153–13159.
[48] J.H. Schiller, G. Bittner, B. Storer, J.K. Willson, Synergistic antitumor effects of tumor necrosis factor and gamma-interferon on human colon carcinoma cell lines, Cancer Res. 47 (11) (1987) 2809–2813.
[49] F. Liu, X. Hu, M. Zimmerman, J.L. Waller, P. Wu, A. Hayes-Jordan, D. Lev, K. Liu, G.S. Wu, TNFα cooperates with IFN-γ to repress Bcl-xL expression to sensitize metastatic colon carcinoma cells to TRAIL-mediated apoptosis, PLoS ONE 6 (1) (2011) e16241.
[50] L. Boland, A.J. Burand, A.J. Brown, D. Boyt, V.A. Lira, J.A. Ankrum, IFN-γ and TNF-α Pre-licensing Protects Mesenchymal Stromal Cells from the Pro-inflammatory Effects of Palmitate, Mol. Ther. 26 (3) (2018) 860–873.
[51] Y. Song, H. Dou, X. Li, X. Zhao, Y. Li, D. Liu, J. Ji, F. Liu, L. Ding, Y. Ni, Y. Hou, Exosomal miR-146a Contributes to the Enhanced Therapeutic Efficacy of Interleukin-1β-Primed Mesenchymal Stem Cells Against Sepsis, Stem Cells 35 (5) (2017) 1208–1221.
[52] K.N. Sivanathan, D. Rojas-Canales, S.T. Grey, S. Gronthos, P.T. Coates, Transcriptome Profiling of IL-17A Preactivated Mesenchymal Stem Cells: A Comparative Study to Unmodified and IFN- Modified Mesenchymal Stem Cells, Stem Cells Int. 2017 (2017) 1025820.
[53] H.-Y. Cheng, M.R. Anggelia, C.-H. Lin, C.-F. Lin, Preconditioned Mesenchymal Stromal Cells to Improve Allotransplantation Outcome, Cells 10 (9) (2021) 2325, https://doi.org/10.3390/cells10092325.
[54] D. Mérino, N. Lalaoui, A. Morizot, E. Solary, O. Micheau, TRAIL in cancer therapy: present and future challenges, Expert Opin. Ther. Targets 11 (10) (2007) 1299–1314.
[55] T. Gura, How TRAIL kills cancer cells, but not normal cells, Science 277 (5327) (1997) 768.
[56] M. van Dijk, A. Halpin-McCormick, T. Sessler, A. Samali, E. Szegezdi, Resistance to TRAIL in non-transformed cells is due to multiple redundant pathways, Cell Death Dis. 4 (7) (2013) e702.
[57] S.K. Lim, B.Y. Khoo, An overview of mesenchymal stem cells and their potential therapeutic benefits in cancer therapy, Oncol. Lett. 22 (5) (2021) 785.
[58] E.A. Kimbrel, R. Lanza, Next-generation stem cells - ushering in a new era of cell-based therapies, Nat. Rev. Drug Discov. 19 (7) (2020) 463–479.
[59] A. Mohr, R. Zwacka, The future of mesenchymal stem cell-based therapeutic approaches for cancer - From cells to ghosts, Cancer Lett. 414 (2018) 239–249.
[60] O. Levy, W.N. Brennen, E. Han, D.M. Rosen, J. Musabeyezu, H. Safaee, S. Ranganath, J. Ngai, M. Heinelt, Y. Milton, H. Wang, S.H. Bhagchandani, N. Joshi, N. Bhowmick, S.R. Denmeade, J.T. Isaacs, J.M. Karp, A prodrug-doped cellular Trojan Horse for the potential treatment of prostate cancer, Biomaterials 91 (2016) 140–150.
[61] S. Amano, S. Li, C. Gu, Y. Gao, S. Koizumi, S. Yamamoto, S. Terakawa, H. Namba, Use of genetically engineered bone marrow-derived mesenchymal stem cells for glioma gene therapy, Int. J. Oncol. 35 (6) (2009) 1265–1270.
[62] A. Nowakowski, K. Drela, J. Rozycka, M. Janowski, B. Lukomska, Engineered Mesenchymal Stem Cells as an Anti-Cancer Trojan Horse, Stem Cells Dev. 25 (20) (2016) 1513–1531.
[63] D.S. Chulpanova, K.V. Kitaeva, L.G. Tazetdinova, V. James, A.A. Rizvanov, V. V. Solovyeva, Application of Mesenchymal Stem Cells for Therapeutic Agent Delivery in Anti-tumor Treatment, Front. Pharmacol. 9 (2018) 259.
[64] R. Yu, L. Deedigan, S.M. Albarenque, A. Mohr, R.M. Zwacka, Delivery of sTRAIL variants by MSCs in combination with cytotoxic drug treatment leads to p53-independent enhanced antitumor effects, Cell Death Dis. 4 (2) (2013) e503.
[65] J.A. Pawitan, T.A. Bui, W. Mubarok, R.D. Antarianto, R.W. Nurhayati, I.H. Dilogo, D. Oceandy, Enhancement of the Therapeutic Capacity of Mesenchymal Stem Cells by Genetic Modification: A Systematic Review, Front. Cell Dev. Biol. 8 (2020) 587776.